AD_____

Award Number: DAMD17-98-1-8583

TITLE: Unique G-rich Oligonucleotides Which Inhibit the Growth of Prostatic Carcinoma Cells

PRINCIPAL INVESTIGATOR: Donald M.Miller, M.D., Ph.D.
Paula J. Bates, Ph.D.
John O. Trent, Ph.D.

CONTRACTING ORGANIZATION: University of Louisville
Louisville, Kentucky 40202

REPORT DATE: July 2001

TYPE OF REPORT: Annual

PREPARED FOR: U.S. Army Medical Research and Materiel Command
Fort Detrick, Maryland 21702-5012

# REPORT DOCUMENTATION PAGE

*Form Approved*
*OMB No. 074-0188*



| 1. AGENCY USE ONLY (Leave blank) | 2. REPORT DATE | 3. REPORT TYPE AND DATES COVERED |
|---|---|---|
| | July 2001 | Annual (1 Sep 99 - 30 Jun 01) |

**4. TITLE AND SUBTITLE**

Unique G-rich Oligonucleotides Which Inhibit the Growth of Prostatic Carcinoma Cells

**5. FUNDING NUMBERS**

DAMD17-98-1-8583

**6. AUTHOR(S)**

Donald M.Miller, M.D., Ph.D.
Paula J. Bates, Ph.D.
John O. Trent, Ph.D.

**7. PERFORMING ORGANIZATION NAME(S) AND ADDRESS(ES)**

University of Louisville
Louisville, Kentucky 40202

E-Mail: dkkonz01@louisville.edu

**8. PERFORMING ORGANIZATION REPORT NUMBER**

**9. SPONSORING / MONITORING AGENCY NAME(S) AND ADDRESS(ES)**

U.S. Army Medical Research and Materiel Command
Fort Detrick, Maryland 21702-5012

**10. SPONSORING / MONITORING AGENCY REPORT NUMBER**

**11. SUPPLEMENTARY NOTES**

Report contains color

**12a. DISTRIBUTION / AVAILABILITY STATEMENT**

Approved for Public Release; Distribution Unlimited

**12b. DISTRIBUTION CODE**

**13. Abstract *(Maximum 200 Words)*** *(abstract should contain no proprietary or confidential information)*

This proposal was based on our original observation that certain G-rich oligonucleotides (GROs) inhibited the growth of cultured prostate cancer cells. The sequences of the active oligonucleotides led us to hypothesize that GROs could form G-quartet containing structures that bind to specific cellular proteins. The overall goal of this proposal was to characterize the structure and mechanism of these novel oligonucleotides. In the first half of this study, the hypotheses regarding G-quartet formation and protein binding were confirmed, and a protein called nucleolin was identified as the tentative target of GROs. During the current reporting period, we have completed the remaining studies in the Phase I proposal. Key results in this period include the following: (1) Structure determination of an active GRO by molecular modeling supported by biophysical data, (2) Demonstration of apoptosis induction in GRO-treated prostate cancer cells, (3) Confirmation of nucleolin as a GRO binding protein and extension of the correlation between GRO activity and ability to bind to nucleolin, and (4) Completion of TRAP assays showing the inability of GROs to inhibit telomerase. In summary, all of the studies proposed in Phase I have been successfully completed or addressed by alternative approaches. This study has produced considerable data to support GROs as potential therapeutic agents for prostate cancer.

| 14. Subject Terms (keywords previously assigned to proposal abstract or terms which apply to this award) | 15. NUMBER OF PAGES |
|---|---|
| experimental therapeutics, oligonucleotides, prostate cancer, nucleolin, G-quartets, quadruplex, structure, non-antisense | 32 |
| | 16. PRICE CODE |

| 17. SECURITY CLASSIFICATION OF REPORT | 18. SECURITY CLASSIFICATION OF THIS PAGE | 19. SECURITY CLASSIFICATION OF ABSTRACT | 20. LIMITATION OF ABSTRACT |
|---|---|---|---|
| Unclassified | Unclassified | Unclassified | Unlimited |

## Table of Contents

# Annual Report for DAMD17-98-1-8583: June 2000 - June 2001

## INTRODUCTION

The proposed research was based on our discovery of novel G-rich oligonucleotides (GROs) that have antiproliferative activity against prostate cancer and other malignant cell lines (1). The goal of this study was to investigate the structure and mechanism of these novel oligonucleotides, which have potential as new therapeutic agents for prostate cancer. The specific aims of the Phase I proposal were:

1. Quantitate the activity of GROs in cultured cells, and examine selectivity, reversibility, and apoptosis.
2. Determine stability, uptake and intracellular localization of GROs.
3. Characterize the structure of antiproliferative GROs and identify biologically active species.
4. Identify and characterize GRO-binding proteins.
5. Use combinatorial techniques to identify new therapeutic oligonucleotides.
6. Characterize inhibition of telomerase by GROs.

## BODY

The progress on each task outlined in the Statement of Work is detailed below:

*Task 1*: To quantitate the antiproliferative activity, induction of apoptosis, reversibility of growth inhibition, and selectivity for malignant cells, by characterizing:

*a.* The ability of GRO15A and GRO29A to inhibit the growth of prostate carcinoma cells (months 1-4)

*b.* The reversibility of growth inhibition (months 1-4)

*c.* The induction of apoptosis (months 4-8)

*d.* The selectivity for malignant cells (months 4-8).

*Progress:* Previously, we had demonstrated antiproliferative activity in DU145 and PC-3 prostate cancer cells. We have now determined that $GI_{50}$ values (concentration required for 50% growth inhibition) for these cell lines for a single dose of GRO29A added directly to the culture medium to be 3 and 5 μM respectively. We have since determined that activity can be significantly improved achieved by annealing GRO in KCl containing buffer to promote G-quartet formation (2). Using this approach, complete inhibition of DU145 cell proliferation can be achieved with a single dose of 5 μM GRO (Figure 1A). GRO15A did not have significant antiproliferative activity using a single dose, and therefore was not pursued further. We also determined that an unmodified DNA analog of GRO29A (GRO26B, 5'-GGTGGTGGTGGTTGTGGTGGTGGTGG) has slightly higher activity (Figure 1B) compared to the original GRO29A and has used this for some subsequent studies. To address reversibility, cells were incubated with GRO for specified times, washed thoroughly to remove GRO, and replaced in the incubator to grow for several more days. In general, short incubations with GRO (4 h) had no effect on cell growth whereas longer incubation (48 h) led to a significant decrease in cell growth even after removal of the oligonucleotide. Although previously we had not specifically detected apoptosis, more detailed experiments revealed clearly the induction of apoptosis in prostate cancer cells. Figure 1C shows that TUNEL (terminal transferase dUTP nick end labeling) staining for fragmented DNA is clearly positive in DU145 prostate cancer cells treated with active GRO (29A) but not control oligonucleotide (15B). Tumor selectivity is a critical issue for any potential therapeutic agent, but unfortunately is rather difficult to address because of the lack of normal cells as controls. However, we were able to show that GROs had much greater activity against cell lines derived from solid tumors and leukemias compared to normal cells such as skin fibroblasts or a mouse mast cell line, which has similar characteristics to hematopoietic progenitor cells (Figure 1D).

*Task 2:* To determine the stability, uptake, and intracellular localization of GRO15A and GRO29A.

*a.* Characterization of GRO stability in serum-containing medium (months 1-4)
*b.* Uptake by prostate carcinoma cells (months 4-8)
*c.* Intracellular localization of GROs (months 8-12)
*d.* Obtain or prepare transfection reagents

*Progress:* This task has been successfully completed. Stability experiments were carried out as described in the original proposal by incubating 5'-$^{32}$P-labeled GROs in serum-containing medium. The results of these experiments showed that GRO29A, even without a 3'-amine modification, has remarkable stability. Figure 2B shows that whereas an unmodified DNA oligonucleotide with a random sequence is degraded within one hour, the unmodified DNA analog of GRO29A is completely intact after 5 days in serum-containing medium. This suggests that the GROs will be sufficiently stable for *in vivo* use without the requirement for expensive backbone or terminal modifications. Previously, we had assessed cellular uptake using 5'-$^{32}$P-labeled oligonucleotides (1), which showed no diffrences between uptake of G-rich, C-rich, or mixed base sequences. However, because we were concerned that the 5'-phosphate could be enzymatically removed, additional uptake experiments were carried out using 5'-fluorescein (FITC)-labeled oligonucleotides. These experiments led to different results, suggesting that active GROs are much more efficiently internalized than inactive GROs or C-rich and mixed base sequences (Figure 2A). We propose that both the enhanced stability and uptake of active GROs are related to G-quartet formation, and further, that the efficient uptake of GROs may be due to enhanced binding to nucleolin on the surface of prostate cancer cells.

*Task 3:* To characterize the structure of GRO15A and GRO29A and to identify the biologically active conformations.

*a.* Electrophoretic characterization of GRO structures (months 1-12)
*b.* NMR structure of GRO15A and GRO29A (months 12-24)
*c.* Molecular modeling studies of GRO15A and GRO29A (months 24-30)

*Progress:* The structure of GRO29A and its structural analog GRO26B have been determined by molecular modeling and confirmed by biophysical studies (GRO15A was not pursued because it is much less active). Preliminary NMR studies have been carried out and the solution structure of GRO26B should soon be completed. The high thermal (melting temperature of 76°C for GRO26B) and biological stability suggests that GROs contain stabilizing motifs such as G quartets. GRO29B/GRO29A could potentially form quadruplex consisting of four, two or one strand (tetramer, dimer, or monmer, Figure 3A). Native polyacrylamide electrophoresis of GRO26B and GRO29A, shown in Figure 3B, showed that the GROs formed predominantly a single species in potassium, but multiple species in sodium. Because the presence of potassium greatly enhanced GRO activity compared to sodium (Figure 1A), we conclude that the active species is present in the faster migrating band. Interestingly, this band migrates at the same location as denatured GRO or single stranded 26-mer, suggesting that it may be a monomer or a very compact dimer. The latter possibility was confirmed by ultracentifugation studies, which showed a molecular mass corresponding to two strands of GRO, and by the absence of antiproliferative activity in a truncated GRO (5'-GGTGGTGGTTGTGGTGGTGG) that should form the monomer shown in Figure 3A equally as well as 26B, but produce a destabilized dimer. The molecular structure of the GRO26B dimer is shown in Figure 3C. The proposed experiments to replace guanosine with 7-deazaguanosine (which cannot form G-quartets) were also carried out. However, the replacement of two (the maximum for practical synthesis reasons) of the guanosines with 7-deazaG was insufficient to prevent formation of the G-quartet structure. In retrospect, this is unsurprising because this represents disruption of only 2 hydrogen bonds out of a total of 64.

*Task 4*: To identify and characterize proteins binding to GRO15A and GRO29A.

*a.* Identification of GRO binding proteins by electrophoretic mobility shift assays (EMSA) and BIAcore capture (months 12-18)
*b.* microsequence analysis (months 18-24)
*c.* demonstration of intracellular binding to GROs (months 24-30)

*Progress:* Previously, we had identified nucleolin as a GRO binding protein whose binding to GROs predicted their antiproliferative activity and provided data to support the binding of GROs to nucleolin in cells (1). We have now extended the correlation between nucleolin binding and activity to include more G-rich sequences (see Task 5; Figure 4). In addition, independent studies (DAMD-01-1-0067 to the co-investigator) have shown that active GROs specifically bind to nucleolin via two RNA binding domains and the RGG C-terminal domain. Using biotinylated GRO or control oligonucleotides, we have captured oligonucleotide-binding proteins using streptavidin coated magnetic beads and identified specific GRO-binding proteins by silver-staining proteins separated by SDS-polyacrylamide gel electrophoresis. With this technique, we were able to detect 14 proteins that bound to an active GRO (29A) but not an inactive GRO (15B). One of these was unambiguously identified by mass spectrometry as nucleolin, and several others were identified as proteins containing RNA binding domains and RGG regions. The relevance of these other GRO-binding proteins is currently being investigated.

*Task 5:* To use combinatorial methods to identify new therapeutic oligonucleotides that have a similar mechanism of action.

*a.* Development of the SURF technique to identify oligonucleotides with maximal activity (months 12-24)
*b.* SELEX techniques to identify oligonucleotides which bind to uPA (months 18-30)

*Progress:* As stated in the previous report, this overly ambitious aim was replaced by an alternative approach of investigating the activity of quadruplex forming oligonucleotides whose structures had previously been characterized by NMR or crystallography. A manuscript is in preparation describing the results of these studies. To summarize these studies, we found that G-quartet formation (although necessary) is not sufficient for antiproliferative activity, and that no simple structure-activity exists. We also confirmed that nucleolin binding is the best factor to predict antiproliferative activity. Figure 4 shows the characteristics of these oligonucleotides, their ability to inhibit the growth of DU145 prostate cancer cells, and their ability to compete for the GRO binding protein (nucleolin) in a mobility shift assay. These results highlight the strong correlation between activity and the ability to bind to nucleolin. It is our current hypothesis that nucleolin is recognizing the shape of the quadruplex groove, which may be similar in quadruplexes with different sequences, rather than the G-quartet itself or the loop region.

*Task 6:* To characterize the ability of GRO15A and GRO29A to inhibit telomerase.

*a.* Development of telomerase assays (months 1-6)
*b.* Measurement of telomerase inhibition (months 6-18) and binding (months 18-30) by GRO

*Progress:* Following the identification of nucleolin as the GRO binding protein, it was felt that telomerase was an unlikely target of GROs. This was confirmed by successful completion of the proposed experiments to measure telomerase activity in GRO treated cells using a commercial TRAP (telomere repeat amplification protocol) assay. These are shown in Figure 5 and indicate that treatment of cells with an antiproliferative GRO does not inhibit telomerase activity.

## KEY RESEARCH ACCOMPLISHMENTS

The following is a list of significant results and achievements for June 2000 - June 2001:

- Identified unmodified oligonucleotide GRO26B as lead compound for further development (*Fig. 1*)
- Demonstrated tumor selectivity in cell lines (*Fig. 1*)
- Demonstrated induction of apoptosis by GROs in prostate cancer cells (*Fig. 1*)
- Molecular structure of GRO26B determined by molecular modeling (*Fig. 3*)
- Showed enhanced cell uptake and remarkable resistance to nuclease digestion of GROs (*Fig. 2*)
- Confirmed nucleolin as a GRO binding protein and showed for a larger set of GROs that nucleolin binding affinity predicts antiproliferative activity (*Fig. 4*)
- Determined that GRO treatment does not inhibit telomerase activity (*Fig. 5*)

## REPORTABLE OUTCOMES

Manuscripts: The data generated during this reporting period were included in the following:

1. Xu X, Hamhouyia F, Thomas SD, Burke TJ, Girvan AC, McGregor WG, Trent JO, Miller DM, Bates PJ. Inhibition of DNA replication and induction of S phase cell cycle arrest by G-rich oligonucleotides. *J. Biol. Chem.* 2001, **276**, 43221-43230.
2. Dapic V, Bates PJ, Trent JO, Rodger A, Thomas SD, Miller DM. Antiproliferative activity of G-quartet-forming oligonucleotides with backbone modifications. *Biochemistry* 2002, **41**, 3676-3685.
3. Dapic V, Abdomerovic V, Marrington R, Peberdy J, Rodger R, Trent JO, Bates PJ. Biophysical and biochemical properties of quadruplex oligonucleotides. *Manuscript submitted.*

Abstracts and meeting presentations:

1. Xu X, Bates PJ, Thomas SD, Miller DM. Inhibition of DNA Synthesis in Prostate Cancer Cells by Novel G-Rich Oligonucleotides. *American Association of Cancer Research 92nd Annual Meeting* April 2001, New Orleans, USA.
2. Dapic V, Bates PJ, Trent JO, Thomas SD, Miller DM. Antiproliferative Activity of G-Quartet Forming Oligonucleotides with Backbone and Sugar Modifications. *American Association of Cancer Research 92nd Annual Meeting*, April 2001, New Orleans, USA

Research grants awarded based on preliminary data generated by this award:

1. Phase II Award (DAMD17-98-1-8583 to D. Miller) "G-rich Oligonucleotides as Novel Therapeutic Agents for Prostate Cancer"
2. New Investigator Award (DAMD-01-1-0067 to P. Bates) "Mechanism of Action of Novel Antiproliferative Oligonucleotides"
3. National Cancer Institute Exploratory Grant (R21 CA 91113 to P. Bates) "Nucleolin as a Novel Target for Cancer Drug Discovery"

## CONCLUSIONS

The studies outlined in the Phase I proposal have been successfully carried out. The results confirm that GROs have potent antiproliferative effects on cell lines derived from prostate carcinoma but not normal cells, and are therefore promising candidates as novel therapeutic agents. GRO26B is an unmodified phosphodiester oligonucleotide that forms a two-stranded structure stabilized by G-quartets. This unique structure gives it remarkable biological stability and efficient cell penetration that make it suitable for use *in vivo*. GRO26B apparently works by a novel mechanism that involves binding to nucleolin protein.

## REFERENCES

1. P. J. Bates *et al.* (1999), *J. Biol. Chem.* **274,** 26369-26377
2. V. Dapic *et al.* (2002), *Biochemistry* **41**, 3676-3685 (manuscript attached).

*Figure 1: Activity, Selectivity and Induction of Apoptosis by GROs*

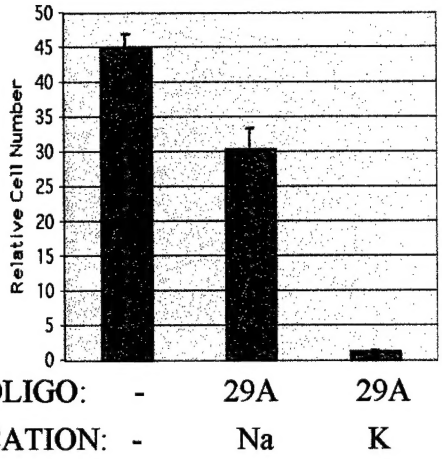


(A) Effect of pre-annealing condition on antiproliferative activity of GRO29A against DU145 prostate cancer cells.

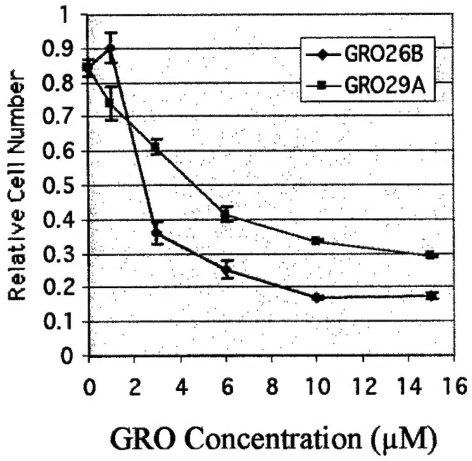


(B) Comparison of antiproliferative activity of GRO29A and its shorter, unmodified analog GRO26B (in HeLa cells).

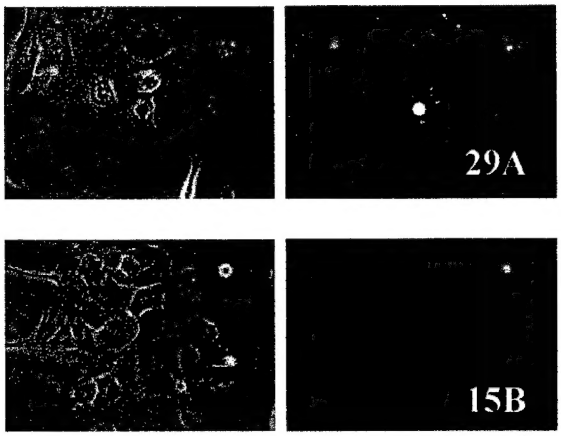


(C) Phase contrast (left) and TUNEL (right) staining of DU145 cells treated with GRO29A or inactive control (15B)

| *Cell Line* | *Cell Type* | *$GI_{50}$ (μM)* |
|---|---|---|
| DU145 | Prostate Cancer | 3 |
| PC3 | Prostate Cancer | 5 |
| MDA-231 | Breast Cancer | 3 |
| HeLa | Cervical Cancer | 6 |
| HS27 | Normal skin | > 10 |
| K562 | Leukemia | 3 |
| Meg-01 | Leukemia | 2 |
| 10P2 | Normal cell | >10 |

(D) Sensitivity of normal and malignant cells to GRO29A. $GI_{50}$ is the concentration required for 50% growth inhibition.

*Figure 2: Stability and Cellular Uptake of GROs*

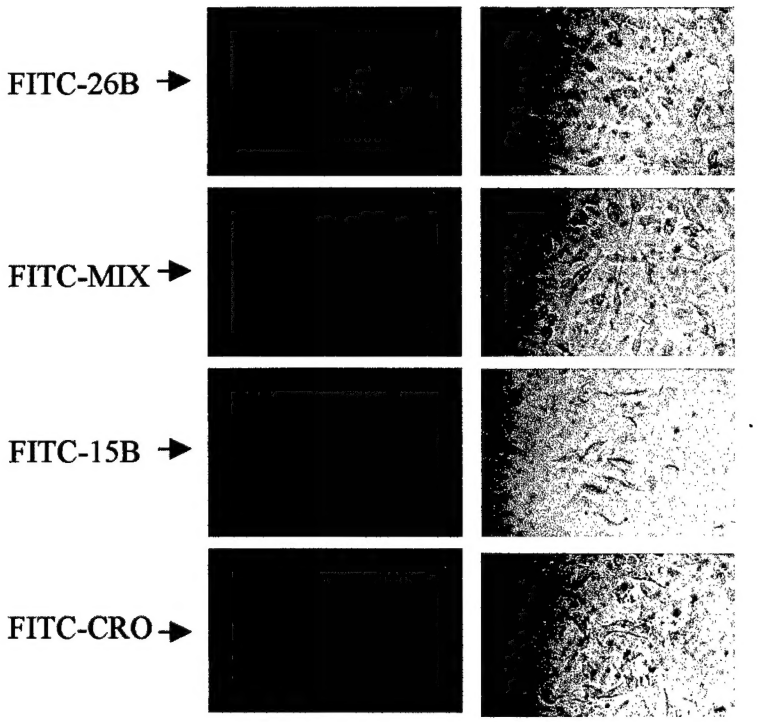


(A) Uptake of FITC-labeled oligonucleotides into DU145 cells (48 h incubation). Sequences corresponded to active GRO (29A), inactive GRO (15B), inactive C-rich analog (CRO), or inactive mixed sequence (MIX).

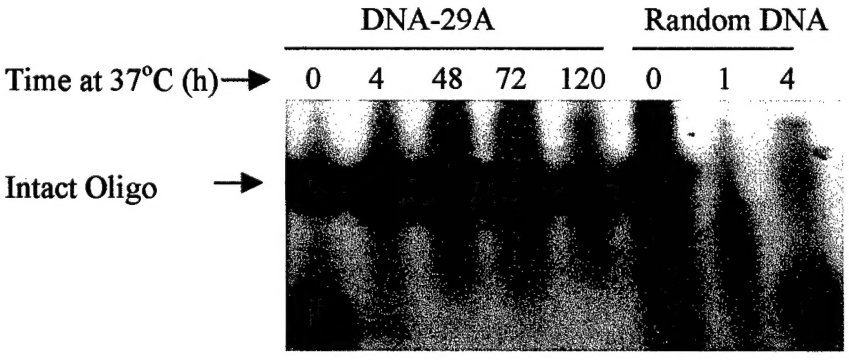


(B) Stability of 5'-radiolabeled oligonucleotides in cell culture medium containing 10 % fetal calf serum. DNA-29A is the 3'-unmodified analog of GRO29A, and Random DNA is a mixed sequence oligonucleotide with no secondary structure.

*Figure 3: Molecular Structure of GRO26B/GRO29A*

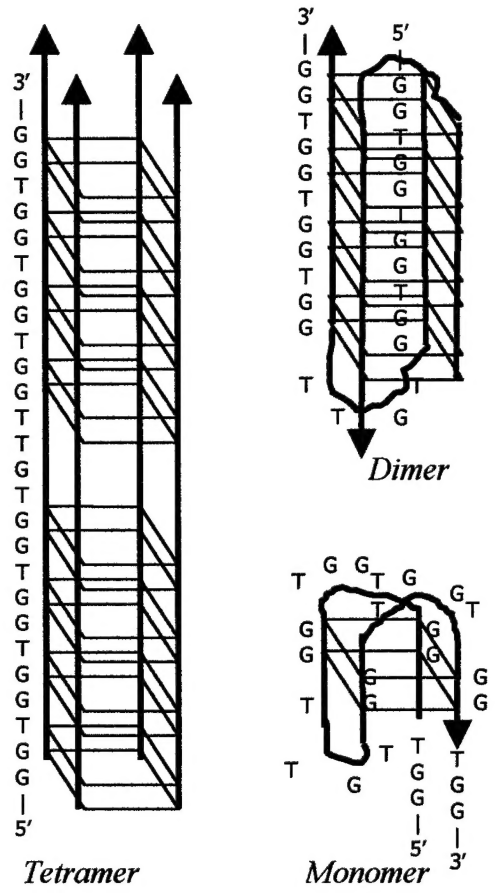


(A) Quadruplex structures stabilized by G-quartets that could potentially be formed by GRO26B and GRO29A.

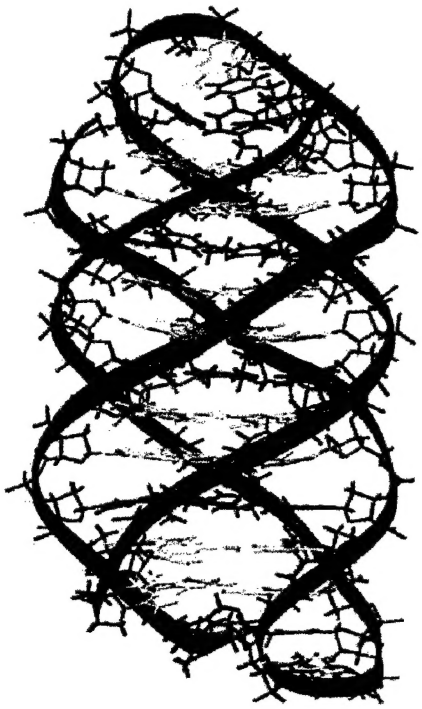

(C) Molecular model of GRO26B dimer.

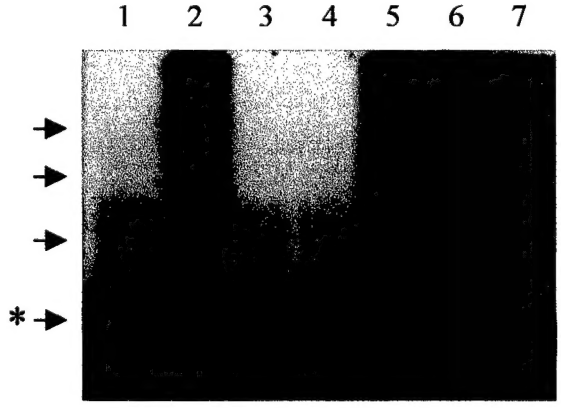


1. TE + 140 mM KCl, 1.5 mM $MgCl_2$
2. TE (denatured)
3. TE + 50 mM KCl
4. TE + 300 mM KCl
5. TE + 50 mM NaCl
6. TE + 500 mM NaCl
7. TE + 100 mM LiCl

(B) Native polyacrylamide electrophoresis showing structures formed by GRO26B that has been annealed in various buffers.

*Figure 4: Structure-Activity Studies of Quadruplex Oligonucleotides*

| *Name* | *Type* | *Sequence* | *Origin* |
|---|---|---|---|
| KS-A | Tetramer | TGGGGT | Telomere |
| KS-B | Monomer | GGTTGGTGTGGTTGG | Thrombin aptamer |
| KS-C | Dimer | GGGGTTTTGGGG | Telomere |
| KS-D | (Non-GQ) | GCATGCT | Non-GQ |
| KS-E | Dimer | GCGGTTTGCGG | Fragile X |
| KS-F | Tetramer | TAGG | Telomere |
| KS-G | Dimer | GGGTTTTGGG | Telomere |
| KS-H | Monomer | $G_4TTTTG_4TTTTG_4TTTTG_4$ | Telomere |
| KS-I | Monomer | $TTG_4TTG_4TTG_4TTG_4$ | Telomere |
| 20A | Monomer | GGTTTTGGTTTTGGTTTTGG | Experimental |
| 23A | Monomer | $G_4TTG_4TGTG_4TTG_4$ | Experimental |
| T30 | Monomer | GGGTGGGTGGGTGGGT | Anti-HIV |
| 29A | Dimer | $T_3(GGT)_4TG(TGG)_4$ | Active GRO |
| 15B | ?? | TTGGGGGGGGTGGGT | Control GRO |

(A) Table showing sequences and characteristics of quadruplex oligonucleotides. All structures had been previously characterized by NMR and/or crystallography.

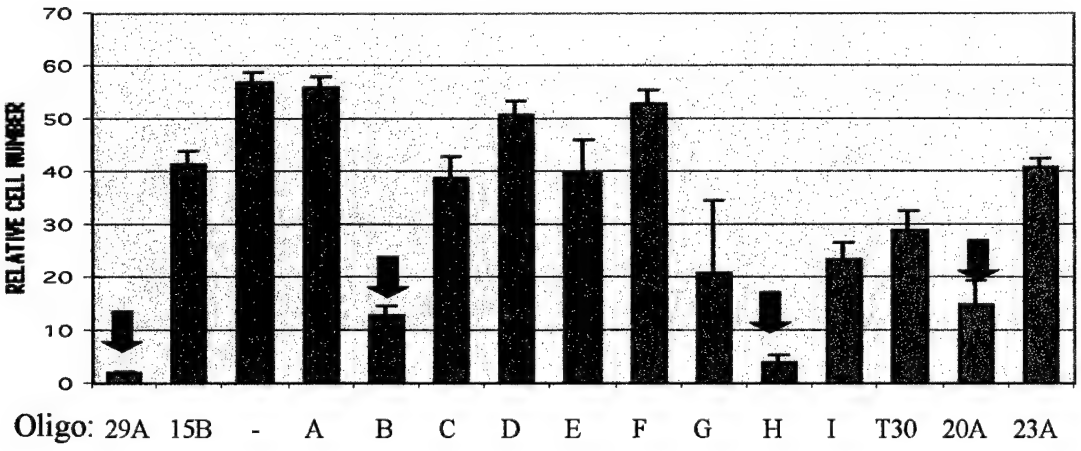


(B) Antiproliferative activity of oligonucleotides. DU145 prostate cancer cells were treated with a single dose (5 μM final concentration) of oligonucleotide and assayed after 7 days.

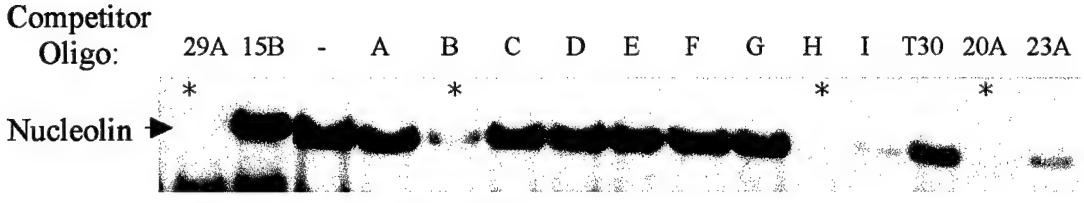


(C) Nucleolin binding of oligonucleotides assessed by competition mobility shift assay (1). Binding to nucleolin is indicated by the disappearance of the band (*) formed by incubating HeLa nuclear extracts with a telomere oligonucleotide.

*Figure 5: Inability of GRO to Inhibit Telomerase Activity*

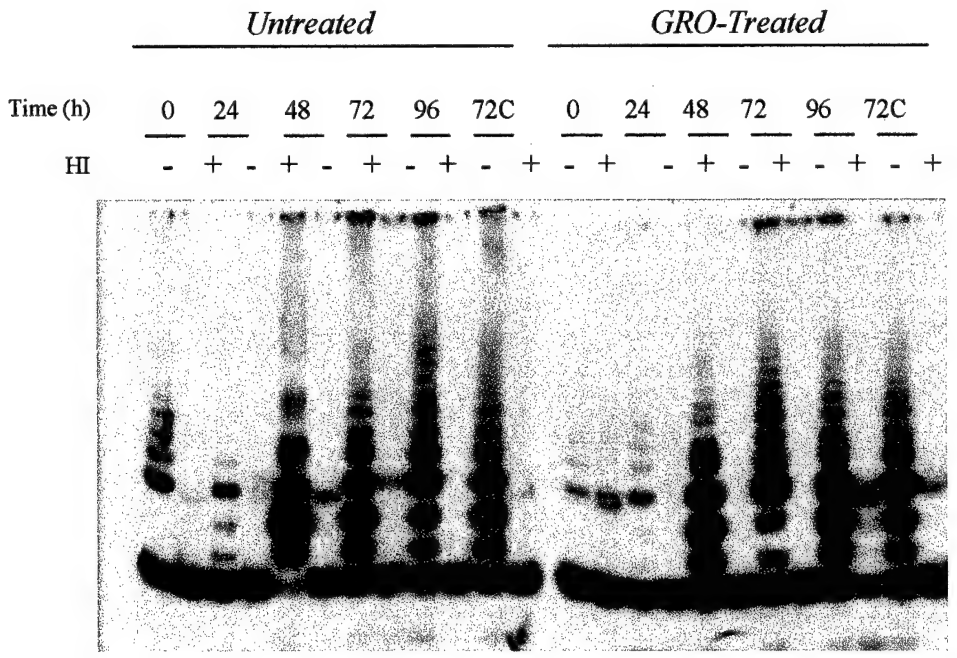


The TRAP assay for telomerase activity was carried out using extracts from untreated or GRO-treated cells. As a control, some extracts were subjected to heat inactivation (HI).

# Antiproliferative Activity of G-Quartet-Forming Oligonucleotides with Backbone and Sugar Modifications†

Virna Đapić,‡,§ Paula J. Bates,§ John O. Trent,§ Alison Rodger,|| Shelia D. Thomas,§ and Donald M. Miller*,§

*Department of Biochemistry and Molecular Genetics, University of Alabama at Birmingham, Birmingham, Alabama 35294, James Graham Brown Cancer Center, University of Louisville, Louisville, Kentucky 40202, and Department of Chemistry, University of Warwick, Coventry CV4 7AL, U.K.*

*Received October 19, 2001; Revised Manuscript Received January 17, 2002*

ABSTRACT: Oligonucleotide-based therapies have considerable potential in cancer, viral, and cardiovascular disease therapies. However, it is becoming clear that the biological effects of oligonucleotides are not solely due to the intended sequence-specific interactions with nucleic acids. Oligonucleotides are also capable of interacting with numerous cellular proteins owing to their polyanionic character or specific secondary structure. We have examined the antiproliferative activity, protein binding, and G-quartet formation of a series of guanosine-rich oligonucleotides, which are analogues of GRO29A, a G-quartet forming, growth-inhibitory oligonucleotide, whose effects we have previously described [Bates P. J., Kahlon, J. B., Thomas, S. D., Trent, J. O., and Miller, D. M. (1999) *J. Biol. Chem. 274*, 26369−26377]. The GRO29A analogues include phosphorothioate (PS29A), 2′-*O*-methyl RNA (MR29A), and mixed DNA/2′-*O*-methyl RNA (MRdG29A) oligonucleotides. We demonstrate by UV spectroscopy that all of the modified analogues form stable structures, which are consistent with G-quartet formation. We find that the phosphorothioate and mixed DNA/2′-*O*-methyl analogues are able to significantly inhibit proliferation in a number of tumor cell lines, while the 2′-*O*-methyl RNA has no significant effects. Similar to the original oligonucleotide, GRO29A, the growth inhibitory oligonucleotides were able to compete with the human telomere sequence oligonucleotide for binding to a specific cellular protein. The less active MR29A does not compete significantly for this protein. On the basis of molecular modeling of the oligonucleotide structures, it is likely that the inactivity of MR29A is due to the differences in the groove structure of the quadruplex formed by this oligonucleotide. Interestingly, all GRO29A analogues, including an unmodified DNA phosphodiester oligonucleotide, are remarkably resistant to nuclease degradation in the presence of serum-containing medium, indicating that secondary structure plays an important role in biological stability. The remarkable stability and strong antiproliferative activity of these oligonucleotides confirm their potential as therapeutic agents.

Synthetic oligodeoxynucleotides (ODNs)[1] can inhibit expression of a particular gene and hold considerable interest to researchers as potential therapeutic agents. The strategies by which the ODNs can exhibit such an effect include antisense [ODN binding to a specific mRNA sequence (*1*)] and antigene, also known as the triplex or triple helix approach [ODN binding to a specific DNA sequence (*2*)].

Recent work has shown that ODNs can also exhibit biological effects, which are unrelated to their sequence-specific interactions with nucleic acids (*3*). In particular, guanosine-rich oligonucleotides are emerging as a new class of nonantisense oligonucleotides whose activity can be related to the formation of G-quartet structure. In addition, G-quartet-forming sequences are of interest for other reasons. First, this structural motif likely has biological significance since genomic sequences from telomeric DNA (*4*), immunoglobulin switch region sequences (*5*), the fragile X repeat sequences (*6*), c-myc oncogene (*7*), and the insulin-linked polymorphic region (*8*) can form G-quartets in vitro. Second, there is also considerable interest in the development of molecules that interact with telomeres (which may form G-quartets in vivo) in order to inhibit telomerase (*9*, *10*), an enzyme thought to be a cancer-specific target (*11*−*13*).

Recently, Bates et al. (*14*) reported that a 29-mer, 3′-modified phosphodiester oligonucleotide (GRO29A), exerts a potent growth inhibitory effect against several cancer cell lines in vitro. This oligonucleotide is stabilized by G-quartet formation, and its activity appears to be related to binding to a cellular protein, possibly nucleolin. It is likely that this growth inhibitory activity is caused by GRO29A inhibition of one or more of the normal functions of the protein. Furthermore, it was shown that the GRO29A specifically arrests the cells in the S-phase of the cell cycle. This arrest is characterized by inhibition of the DNA synthesis (*15*).

† This work was supported by NCI Grants RO1CA42664 and RO1CA54380 and U.S. Army Prostate Research Initiative PC970218.

* To whom correspondence should be addressed. Phone: (502) 562-4369. Fax: (502) 562-4368. E-mail: donaldmi@ulh.org.

‡ University of Alabama at Birmingham.

§ University of Louisville.

|| University of Warwick.

[1] Abbreviations: ODN, oligodeoxynucleotides; GRO, G-rich oligonucleotide; PBS, phosphate-buffered saline; DMEM, Dulbecco's modified Eagle medium; FCS, fetal calf serum; MTT, 3-(4,5-dimethylthiazol-2-yl)-2,5-diphenyltetrazolium bromide; CD, circular dichroism; PBC, periodic boundary conditions; PME, particle mesh Ewald summation; HIV, human immunodeficiency virus.

10.1021/bi0119520 CCC: $22.00 
Published on Web 02/20/2002

Table 1: Synthetic Oligonucleotides

| oligonucleotide | sequence | properties |
|---|---|---|
| GRO29A | 5′-TTT GGT GGT GGT GGT TGT GGT GGT GGT GG-3′ | phosphodiester backbone; 3′-aminoalkyl group modification; deoxyguanosines and deoxythymidines; original antiproliferative oligonucleotide |
| PS29A | 5′-*TTT GGT GGT GGT GGT TGT GGT GGT GGT GG*-3′ | phosphorothioate backbone; deoxyguanonsies and deoxythymidines; analogue of GRO29A |
| MRdG29A | 5′-UUU GGU GGU GGU GGU UGU GGU GGU GGU GG-3′ | 2′-*O*-methyluracil and deoxyguanosines (RNA); chimeric analogue of GRO29A |
| MR29A | 5′-**UUU GGU GGU GGU GGU UGU GGU GGU GGU GG**-3′ | 2′-*O*-methyluracil and 2′-*O*-methylguanosines (RNA); analogue of GRO29A |
| 29A-OH | 5′-TTT GGT GGT GGT GGT TGT GGT GGT GGT GG-3′ | phosphodiester backbone; no 3′ modifications; deoxyguanosines and deoxythymidines; analogue of GRO29A |
| TEL | 5′-TTA GGG TTA GGG TTA GGG TTA GGG-3′ | phosphodiester backbone; human telomere sequence |
| CH1 | 5′-UUU GGU GGU GGU GGU UGU GGU GGU GGU GG-3′ | chimeric 2′-*O*-methyluracil and deoxyguanosine (RNA); **G** at position 17 was replaced with 2′-*O*-methyl G in studies determining the importance of the loop region |
| CH2 | 5′-**UUU GGU GGU GGU GGU UGU GGU GGU GGU GG**-3′ | chimeric 2′-*O*-methyluracil and 2′-*O*-methylguanosine (RNA); *G* at position 17 was replaced with deoxyguanosine in studies determining the importance of the loop region |
| 15B | 5′-TTG GGG GGG GTG GGT-3′ | phosphodiester backbone; 3′-aminoalkyl group modification; deoxyguanosines and deoxythymidines; control G-rich oligonucleotide with negligible antiproliferative activity |
| PS15B | 5′-*TTG GGG GGG GTG GGT*-3′ | phosphorothioate backbone; deoxyguanosines and deoxythymidines; analogue of 15B |
| MR15B | 5′-**UUG GGG GGG GUG GGU**-3′ | 2′-*O*-methyluracil and 2′-*O*-methylguanosines (RNA); analogue of 15B |
| P2C | 5′-TCT AGA AAA ACT CTC CTC TCC TTC CTC CCT CTC CA-3′ | unmodified phosphodiester oligonucleotide; control mixed sequence |

Because phosphodiester oligonucleotides are extremely sensitive to nuclease degradation in biological media, they are usually considered unsuitable for experiments in vivo and in cell culture systems. Most antisense studies have therefore been carried out using modified oligonucleotides, including phosphorothioate derivatives (*16*, *17*). Despite their increased stability, toxicities have been observed in animal studies. The major toxicities are thought to be due to the polyanionic nature of these oligonucleotides, which allows them to bind to numerous cellular proteins. In addition, they appear to be immunostimulatory, inducing the expression of cytokines and chemokines (*17*−*19*). However, despite their limitations, there have been numerous studies reporting sequence-specific effects of phosphorothioate oligonucleotides, and these have resulted in several clinical trials (*20*−*23*). These studies have shown that oligonucleotides can be safely administered to humans.

To fully characterize the antiproliferative activity of G-rich oligonucleotides such as GRO29A, we have examined several analogues with modified sugar−phosphate backbones. Here we present the results of our evaluation of the antiproliferative activity, protein binding, G-quartet formation, and stability in serum-containing medium of these analogues. We have demonstrated that phosphorothioate and mixed DNA/2′-*O*-methyl analogues of GRO29A exhibit strong antiproliferative activity, which is attributed to their ability to bind to the cellular protein, nucleolin, as well as their ability to form stable G-quartet structures. The formation of G-quartets renders these oligonucleotides extremely stable against nuclease degradation, and this stability is maintained without additional modifications. This is the first reported example, to the authors' knowledge, of 2′-*O*-methyl RNA and mixed 2′-*O*-methyl RNA:DNA forming G-quartet-containing structures.

## EXPERIMENTAL PROCEDURES

*Oligonucleotides.* All oligonucleotides were purchased from Oligos Etc. (Wilsonville, OR). The integrity of the oligonucleotides was verified by 5′-radiolabeling followed by analysis on denaturing polyacrylamide gels. Oligonucleotides were resuspended in phosphate-buffered saline (PBS) at a concentration of 500 $\mu$M and annealed by boiling for 5 min and cooling slowly to room temperature.

*Detection of G-Quartets by UV Spectroscopy.* Oligonucleotides were resuspended in Tm buffer (140 mM KCl, 2.5 mM $MgCl_2$, and 20 mM Tris·HCl, pH 8.0) at a final concentration of 2 $\mu$M. Oligonucleotides were annealed by the method described above and were further incubated at 4 °C overnight. Thermal denaturation−renaturation experiments were carried out using an Ultrospec 2000 instrument equipped with a Peltier effect heated cuvette holder and temperature controller (Amersham Pharmacia Biotech). A temperature range of 25−95 °C was used to monitor absorbance at 295 nm at a heating/cooling rate of 0.5 °C/min.

*Circular Dichroism Study.* Oligonucleotides, at a final concentration of 5 $\mu$M or 2.5 $\mu$M, were resuspended in 10 mM sodium phosphate buffer, pH 7.0, containing 0.1 M KCl (final volume, 1 mL), were boiled for 5 min, and annealed at 60 °C for 56 h. Samples were analyzed on a Jasco J-175 spectropolarimeter. Spectra were collected over 16 scans at 100 nm/min, 1 s response time, and 1 nm bandwidth. Cuvettes, 4 mm wide, with black quartz sides to mask the light beam were used for the measurements.

*Cell Growth Assay.* Cells were plated at a density of $10^3$ cells/well in a 96-well plate in Dulbecco's modified Eagle medium (DMEM) supplemented with 10% fetal calf serum (FCS), which has been heat inactivated for 30 min at 55 °C. After 4 h to allow adherence of cells, oligonucleotides were

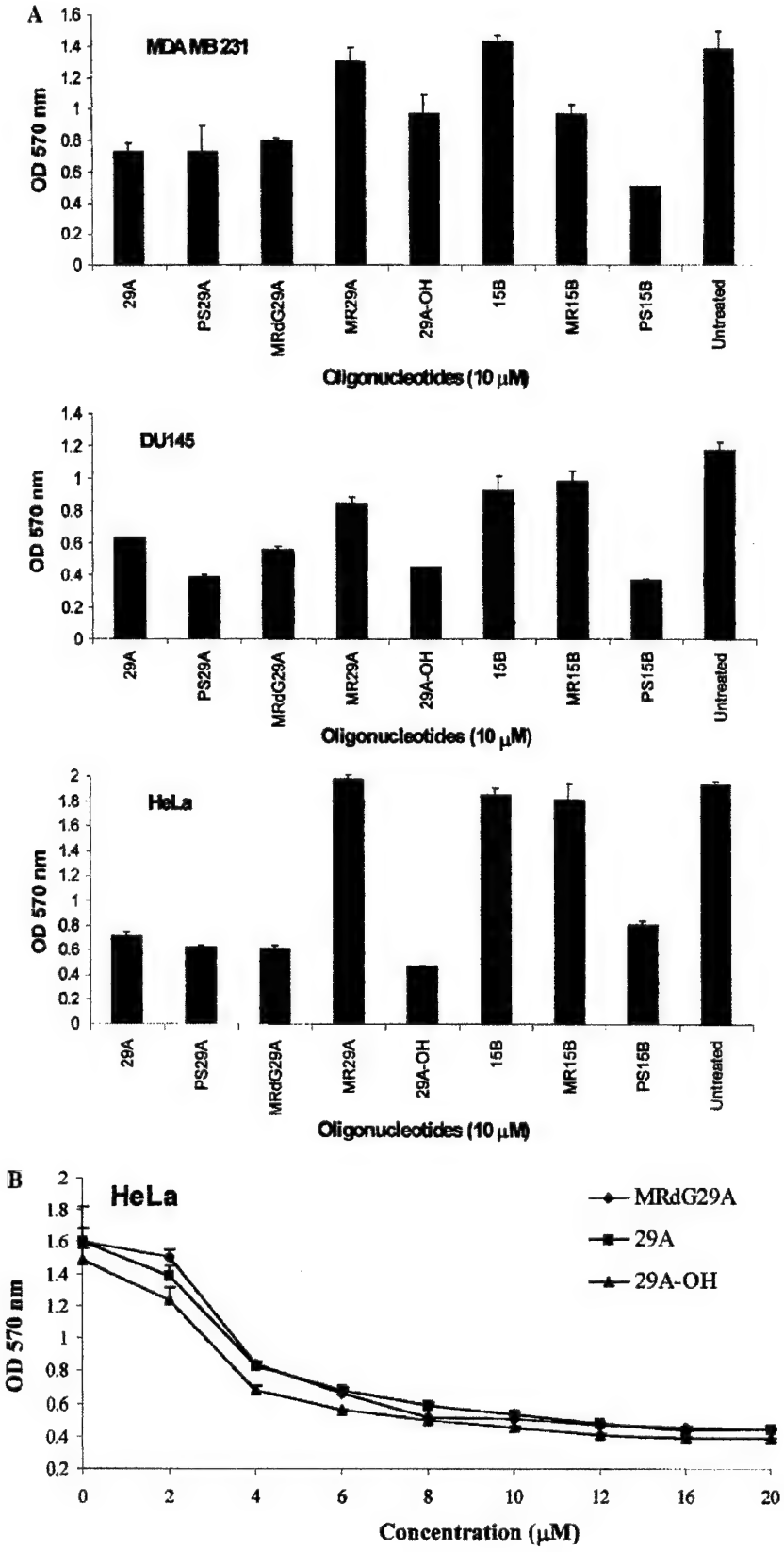


FIGURE 1: Activity of G-rich oligonucleotides in cancer cell lines determined with MTT assay. (A) Cancer cell lines were treated with G-rich oligonucleotides by direct addition of the GRO to the culture medium. The cell type used is shown in the upper left corner of each graph. (B) Dose−response curve for HeLa cells treated with G-rich oligonucleotides. Symbols representing oligonucleotides are shown in the upper right corner of the graph. Experiments for both figures were performed in triplicate, and bars represent the standard error of the data.

added directly to the culture medium to give a final concentration of 10 $\mu$M. Cells were further incubated at 37 °C in 10% $CO_2$. Seven days after the addition of oligonucleotides, cell viability was assayed using the MTT assay (*24*). Culture medium was not replaced during the 7 days. The experiments were performed in triplicate, and bars represent the standard error of the data.

*Electrophoretic Mobility Shift Assay (EMSA).* TEL oligonucleotide was labeled with $^{32}P$ using T4 kinase. Labeled oligonucleotide ($2 \times 10^4$ cpm per reaction, final concentration approximately 1 nM) was preincubated alone or in the presence of an unlabeled competitor oligonucleotide for 30 min at 37 °C. HeLa nuclear extracts (bandshift grade; Promega, Inc., Madison, WI) were added, and samples were incubated for an additional 30 min at 37 °C. Preincubation and binding reactions were carried out in buffer A (20 mM Tris·HCl, pH 7.4, 140 mM KCl, 1 mM dithiothreitol, 0.2 mM phenylmethanesulfonyl fluoride, and 8% v/v glycerol). Electrophoresis was carried out using 5% polyacrylamide gels in TBE buffer (90 mM Tris−borate and 2 mM EDTA).

*Stability of Oligonucleotides in Cell Culture Medium.* Labeled oligonucleotides (total of $10^6$ cpm of each) were incubated in the cell culture medium (DMEM supplemented with 10% FCS, heat inactivated at 55 °C for 30 min) at 37 °C for 0, 4, 48, 72, and 120 h. At each time point, 10 $\mu$L of sample was removed, briefly centrifuged, and quick-frozen by placement in a dry ice/ethanol mixture. Samples were stored at −80 °C until analysis. Prior to analysis, samples were quickly thawed out at 37 °C, and 10 $\mu$L of loading buffer (98% deionized formamide, 10 mM EDTA, pH 8.0, 0.025% bromophenol blue, and 0.025% xylene cyanol FF) was added to each sample. Samples were boiled for 5 min and placed on ice prior to being analyzed by denaturing polyacrylamide gel electrophoresis on a 7 M urea/16% polyacrylamide gel.

*Stability of Oligonucleotides in Cytoplasmic Extracts.* Labeled oligonucleotides ($5 \times 10^5$ cpm of each) were incubated in HeLa S-100 [prepared as previously described (*25*)], 2 $\mu$g total protein, at 37 °C for up to 8 h. At each time point, 10 $\mu$L of sample was removed and quick-frozen as above. Samples were analyzed in the same way as for the culture medium stability experiments.

*Molecular Modeling of GRO29A and Its Analogues MR29A and MRdG29A.* The dimeric chair model of the antiparallel GRO29A structure was generated using the human telomere solution structure (*26*). This final model generated by the protocol below was modified to produce the starting model of the analogous structures, which consequently were examined using the same protocol. The structure was minimized by steepest descents (1000 steps) and Polack−Riberie (2000 steps) conjugated gradient methods. The AMBER* force field and the GB/SA implicit water continuum solvation within Macromodel 7.0 (*27*) were used for all minimization and molecular dynamics calculations. The minimized structure was equilibrated at 300 K for 100 ps (1.5 fs time step) using molecular dynamics. The final structure was generated by averaging a further molecular dynamics production phase of 1 ns, sampling at 1 ps in the last 50 ps, with subsequent minimization. Fully solvated molecular dynamics calculations using AMBER 6.0 with PBC and PME are ongoing and will be reported separately. The molecular surfaces for Figure 5A were generated in INSIGHTII (*28*). Analysis of the grooves of GRO29A, MR29A, and MRdG29A was done using GrooveView (*29*). This program generates the molecular surfaces of the region of interest and provides cross-section slices (1.6 Å apart) of the surface perpendicular to the groove axis (Figure 5B).

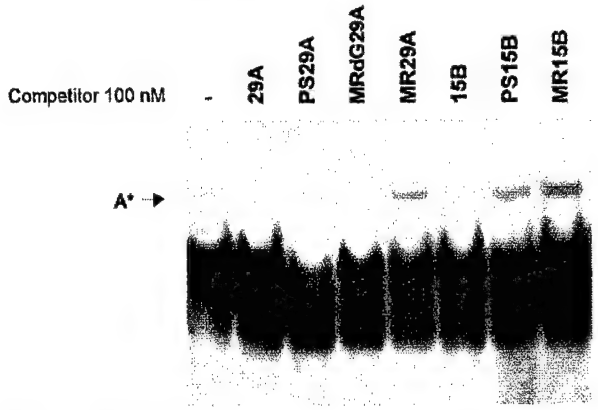


FIGURE 2: Electrophoretic mobility shift assay with 5′-labeled TEL oligonucleotide. Radiolabeled TEL was incubated with nuclear protein extract alone or in the presence of unlabeled, competitor G-rich oligonucleotides and control. Oligonucleotide samples were incubated in buffer A (20 mM Tris·HCl, pH 7.4, 140 mM KCl, 1 mM dithiothreitol, 0.2 mM phenylmethanesulfonyl fluoride, and 8% v/v glycerol) and electrophoresed on 5% polyacrylamide gels in TBE buffer. Band A* represents a complex formed between the TEL and the protein(s), which is competed specifically by active GROs.

## RESULTS

*Modified G-Rich Oligonucleotides Inhibit Cancer Cell Proliferation in Cell Culture.* The oligonucleotides were tested for antiproliferative activity in three cancer cell lines, derived from cervical (HeLa), breast (MDA-MB 231), and prostate (DU 145) carcinomas. The structure and modifications of all oligonucleotides are described in Table 1. These oligonucleotides included a phosphorothioate analogue, a full 2′-*O*-methyl RNA analogue, and an analogue with deoxyguanosines and 2′-*O*-methyluridines. The original GRO29A was the only one with 3′ amino group modification. We also tested 29A-OH, a phosphodiester analogue without the 3′-propylamino group, to determine whether 3′ modification was necessary for oligonucleotide stability. Control oligonucleotides were analogues of GRO15B, which was previously found to have very weak antiproliferative activity (*14*).

Figure 1A demonstrates the growth inhibitory activity of the various oligonucleotides as measured by the MTT assay, which determines the relative number of viable cells. In each of the cell lines tested, we observed that the GRO29A analogues PS29A, MRdG29A, and 29A-OH had similar or greater growth inhibitory activity compared to GRO29A. The analogue containing all 2′-*O*-methyl RNA nucleotides, MR29A, was inactive or had only weak antiproliferative activity. Of the control oligonucleotides, GRO15B had a much weaker antiproliferative effect, as expected, and the 2′-*O*-methyl RNA (MR15B) control had a similar effect. However, the phosphorothioate control (PS15B) had significant antiproliferative effect that equaled or exceeded that of PS29A. Possible explanations for this observation will be discussed below.

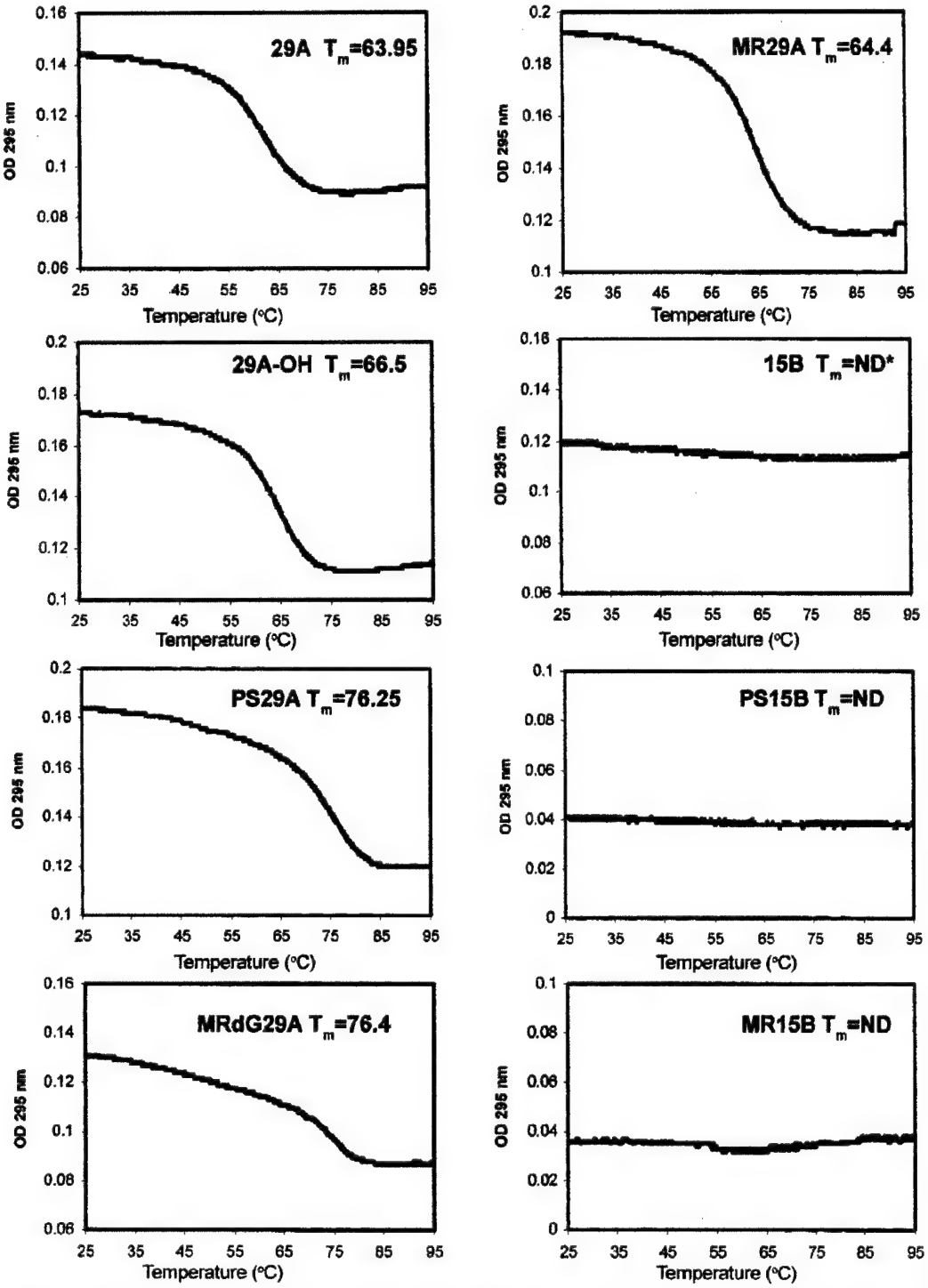


FIGURE 3: G-quartet formation of G-rich oligonucleotides assessed by UV thermal renaturation studies. The oligonucleotide name is shown in the upper right corner of each graph. Experiments were carried out in Tm buffer (20 mM Tris·HCl, pH 8.0, 140 mM KCl, and 2.5 mM $MgCl_2$). ND = not detected.

We also determined the $GI_{50}$ (50% growth inhibition) for the active oligonucleotides. In HeLa cells treated with a single dose of oligonucleotide and assayed after 7 days, the $GI_{50}$ values were similar for GRO29A, MRdG29A, and PS29A (4 $\mu$M; see Figure 1B).

*Relationship between Growth Inhibitory Activity and Protein Binding.* It was previously reported (*14*) that the antiproliferative activity of G-rich oligonucleotides correlated with their ability to bind to a specific cellular protein, which also binds to the human telomere sequence oligonucleotide. To test whether the antiproliferative activity of the GRO29A analogues is also related to binding to this protein, we used a competitive electrophoretic mobility shift assay (EMSA). 5′-Radiolabeled TEL oligonucleotide (a G-quartet-forming oligonucleotide) representing the human telomere sequence was incubated with HeLa nuclear extracts alone or in the

presence of unlabeled competitor oligonucleotide, and the interaction was examined by an EMSA. Figure 2 depicts the formation of the TEL−protein complex and the ability of the unlabeled oligonucleotides to compete for binding to the protein(s). The experiment shows that the GRO29A analogues with antiproliferative activity (PS29A and MRdG29A) were able to compete with TEL for binding with the protein, whereas the inactive analogue, MR29A, was not able to compete for binding. This is indicated by the reduced intensity of band A when active analogues were included. Of the control oligonucleotide analogues, none were able to compete significantly for protein binding. This indicates that the protein is specifically recognizing some characteristic of active GRO29A analogues, rather than simply binding to G-rich oligonucleotides. The obvious exception to the observed correlation between biological activity and binding to the specific protein is PS15B, which has high antiproliferative activity but does not compete for protein binding. We conclude from this that this oligonucleotide is exerting its effect via a mechanism that is different from that of GRO29A and its active analogues. This is unsurprising in light of what is known of the nonspecific effects of phosphorothioate oligonucleotides, which have a much higher level of nonspecific protein binding compared to phosphodiester oligonucleotides (*17*, *19*). Because the PS analogue of GRO29A is able to compete for protein binding, it seems likely that the activity of PS29A stems from a combination of both nonspecific effects and specific GRO29A-like effects.

*Modified G-Rich Oligonucleotides Form G-Quartets.* The failure of MR29A, the 2′-*O*-methyl oligonucleotide, to inhibit the growth of cells may be a result of a number of factors. One explanation would be that the 2′-*O*-methyl RNA could not form G-quartet structures. Alternatively, it may form a G-quartet structure, which is significantly different from that of GRO29A, and therefore would not be a substrate for binding to the active GRO-specific protein.

To investigate the possibility that the 2′-*O*-methyl RNA analogue cannot form G-quartets, we have analyzed G-quartet formation of all GRO29A analogues. A UV thermal denaturation−renaturation method described by Mergny et al. (*30*) was employed for this study. This method is based on the fact that dissociation of antiparallel G-quartets (those formed in folded dimeric or monomeric molecules) leads to decreased absorbance at 295 nm. Figure 3 shows the annealing curves for the oligonucleotides tested. G-quartet formation is indicated with a clear transition, as seen for GRO29A, which has a melting temperature of approximately 63 °C. MRdG29A, MR29A, and PS29A all showed a similar profile to the one observed for GRO29A, with similar or slightly higher $T_m$. This profile was reversible, with a small hysteresis (2−3 °C difference between heating and cooling curves). None of the control GRO15B analogues exhibited transitions consistent with G-quartet formation, even though they contain contiguous runs of guanosines. We also tested the melting of this oligonucleotide by monitoring the absorbance at 260 nm, which would indicate parallel tetrameric quadruplet formation, but that also did not show the presence of G-quartet structure.

*Circular Dichroism Evaluation of G-Quartets.* The method used to detect $T_m$ for the oligonucleotides has been shown to be specific for antiparallel G-quartets. We further wanted to test the folding of GRO29A and its analogues by employing circular dichroism (CD) measurements. It is generally thought that parallel-type G-quartets, when analyzed by CD, have a positive ellipticity maximum at 264 nm and a negative ellipticity minimum at 240 nm, while the antiparallel G-quartet structures have a strong positive maximum between 290 and 295 nm and a minimum at 265 nm (*31*). However, we have found (Bates and Rodger, unpublished data) that some G-quartets known to form in the antiparallel orientation exhibit the classical parallel G-quartet spectra with a positive 264 nm peak. Jing et al. reported a similar finding (*32*), where analysis of a potent anti-HIV oligonucleotide T30177 showed CD spectra consistent with parallel G-quartets. However, this oligonucleotide forms antiparallel G-quartets.

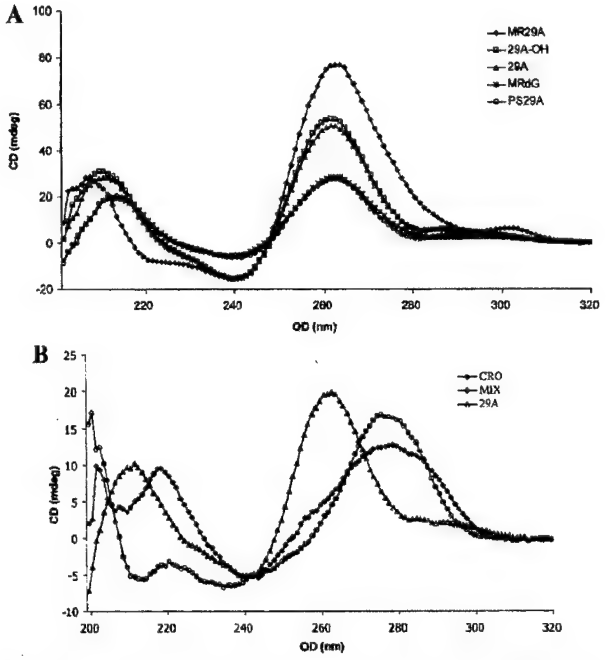


FIGURE 4: (A) CD spectra of MR29A, 29A-OH, 29A, MRdG, and PS29A. CD data were obtained with a 5 $\mu$M strand concentration in the presence of 0.1 M KCl at 25 °C. (B) CD spectra of CRO, mix, and 29A oligonucleotides (2.5 $\mu$M strand concentrations).

G-rich oligonucleotide 29A appears to fall into this category. The CD spectrum (Figure 4A) shows that 29A exhibits a strong 264 nm peak characteristic of G-quartets. This signature peak is absent in mixed sequence or C-rich oligonucleotides (Figure 4B). Figure 4A further shows that all of the GRO29A modified analogues have negative ellipticity minimum at 240 nm and a positive ellipticity maximum at 264 nm. MR29A has a slight shift with an additional minor peak between 300 and 310 nm. The difference is most likely due to the 2′-*O*-methyl groups contributing to the different stacking of G-quartets.

*Molecular Modeling of GRO29A Analogues.* To investigate whether the structure of the G-quartet species formed by inactive MR29A was different from that formed by GRO29A and MRdG29A, we carried out molecular modeling studies. The molecular dynamics simulations produced stable models for GRO29A, MR29A, and MRdG29A, which are consistent with all experimental data (Figure 5A). The models were similar with respect to G-quartet stability and overall structure but had major differences in their topological features. The cross sections of the solvent-accessible surface

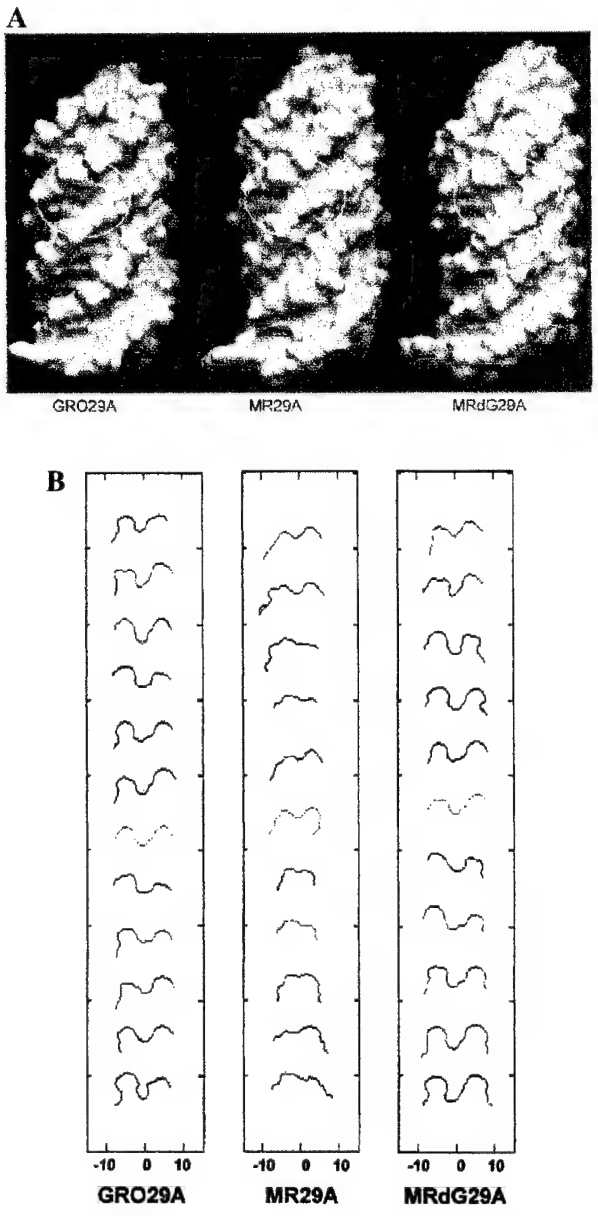


FIGURE 5: Structural studies of G-rich oligonucleotides. (A) Molecular surface representations of the molecular models of GRO29A, MR29A, and MRdG29A. (B) Cross sections of the solvent-accessible surface of the circled regions of (A) generated by GrooveView (*29*).

of the circled regions in Figure 5A are shown in Figure 5B. The quadruplex grooves of GRO29A and MRdG29A had similar characteristics, whereas in the case of MR29A, the depth and shape of the grooves were considerably altered by the effect of the 2′-*O*-methyl sugar substituents of the guanosines. The effect of the 2′-*O*-methyl groups in MR29A is to change the nature of the grooves, thus making the four grooves significantly different. This is typified by the fact that the region of the curve chosen for the analysis does not have the 2′-*O*-methyl groups located in that groove, so the narrowing of the groove is not simply due to "filling" the groove with the substituents. The average depth of this groove region for GRO29A and MRdG29A is approximately 5 Å whereas the groove in MR29A ranges from 0 to 2 Å.

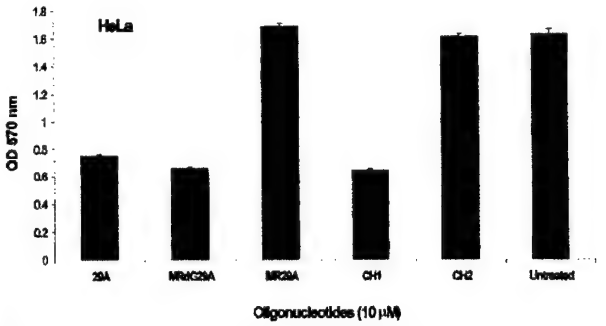


FIGURE 6: Loop region studies. Loop region studies were carried out with chimeric G-rich oligonucleotides. Base substitutions are indicated in Table 1. Activity was assayed using the MTT assay. Experiments were performed in triplicate, and bars represent the standard error of the data.

Table 2: Guanosines in the Quartet Core and Loop Regions

| oligonucleotide | quartet core | loop | activity |
|---|---|---|---|
| GRO29A | deoxyguanosines | deoxyguanosines | ++++ |
| MRdG29A | deoxyguanosines | 2′-*O*-methyl RNA | ++++ |
| MR29A | 2′-*O*-methyl RNA | 2′-*O*-methyl RNA | − |
| CH1 | deoxyguanosines | 2′-*O*-methyl RNA | ++++ |
| CH2 | 2′-*O*-methyl RNA | deoxyguanosines | − |

*Study of the Loop and G-Quartet Region of MR29A and MRdG29A.* To exclude the possibility that the activity of MRdG29A was a result of differences in the loop rather than G-quartet structure, we designed two chimeric oligonucleotides, CH1 and CH2, where CH1 had deoxyguanosines in the G-quartet region and 2′-*O*-methylguanosines in the loop region. Both chimeric oligonucleotides were tested in cell growth assay (MTT) using the HeLa cell line to determine their antiproliferative activity following the substitutions (Figure 6). The activity of CH1 was not diminished due to the change in sequence, while CH2, which had 2′-*O*-methylguanosines in the G-quartet core and deoxyguanosines in the loop region, had no antiproliferative activity (see Table 2). This allowed us to conclude that the loop is unlikely to play a direct role in the activity.

*Stability of G-Rich Oligonucleotides in Serum-Containing Medium and Cellular Extracts.* The poor stability of unmodified oligonucleotides in vivo presents one of the major obstacles in their development as potential therapeutic drugs. Therefore, we investigated the stability of unmodified and modified oligonucleotides in serum-containing medium as well as in cellular extracts.

Figure 7A shows that all of the G-quartet-forming oligonucleotides were stable in serum-containing medium for at least 72 h. We also tested 29A-OH, a phosphodiester analogue of GRO29A without the 3′ modification, and compared it to a random oligonucleotide P2C, which has no detectable secondary structure. The G-quartet forming oligonucleotide, 29A-OH, was stable for over 5 days while the P2C oligonucleotide was degraded within 1 h of being added to the serum-containing medium (Figure 7B). Similar indications of stability were obtained when oligonucleotides were tested in S-100 extracts of HeLa cells (not shown). All G-quartet-forming oligonucleotides were completely undegraded after 8 h at 37 °C in the presence of 2 μg of protein extract.

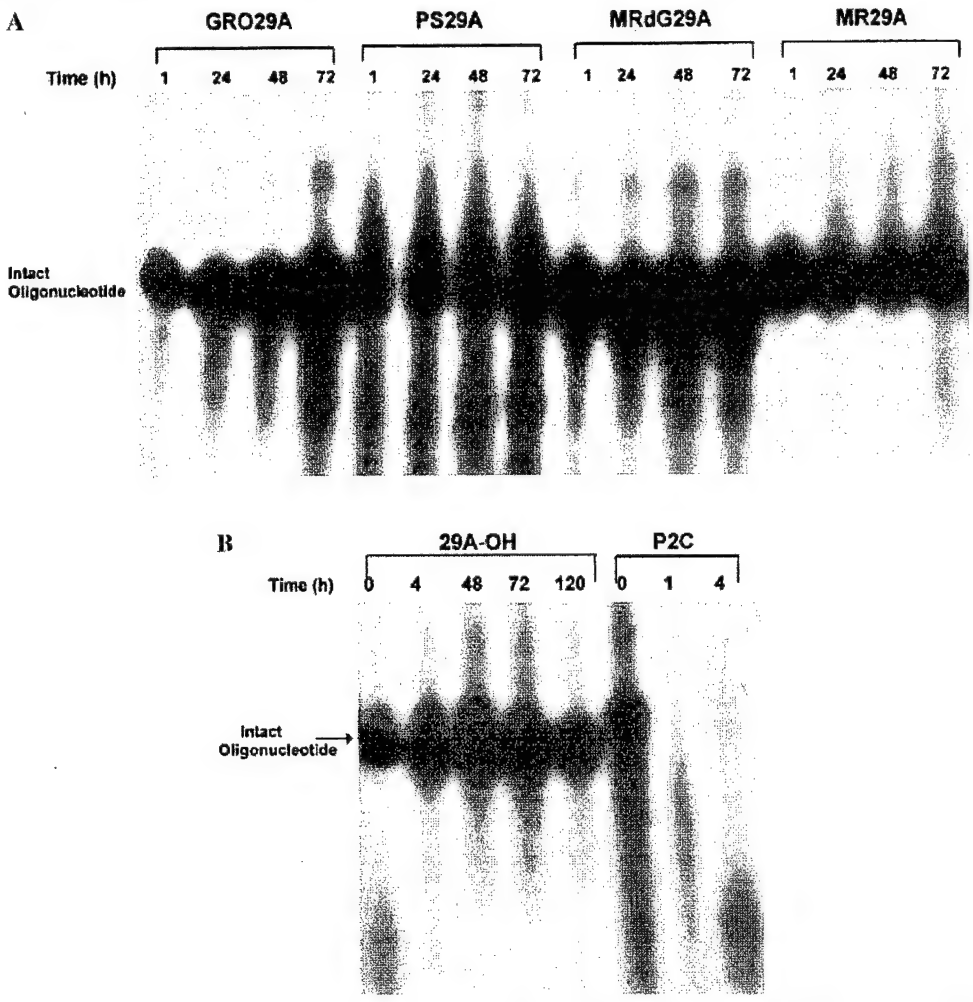


FIGURE 7: Stability of G-rich oligonucleotides in serum-containing medium. (A) 5′-Labeled oligonucleotides were incubated for the times indicated in the presence of culture growth medium (DMEM supplemented with 10% FCS, heat inactivated at 55 °C for 30 min). Samples were analyzed on a denaturing (7 M urea) 16% polyacrylamide gel. (B) 5′-Labeled G-rich oligonucleotide 29A-OH and an unmodified, phosphodiester oligonucleotide, P2C, were incubated for the times indicated in the presence of culture growth medium.

It is most remarkable that 29A-OH, an unmodified phosphodiester oligonucleotide, is stable for over 5 days in serum-containing medium. Since phosphodiester oligonucleotides (e.g., P2C) are generally degraded within minutes under such conditions, it appears that G-quartet formation is extremely important for oligonucleotide stability. Presumably, the folded structure of 29A-OH prevents access by nucleases. It is also possible that the novel structure formed by these oligonucleotides is unrecognized by any helicases, which may unravel them. The high stability of GRO29A and its analogues also suggests that the intact oligonucleotide, rather than a degradation product, is the active species.

In fact, the potential therapeutic success of any oligonucleotide therapy will depend on the ability of the oligonucleotide to remain intact under in vivo conditions. Our results suggest that any of the GRO29A analogues tested would have sufficient stability in vivo to make them therapeutically useful.

Another G-quartet-forming oligonucleotide with a phosphodiester backbone (except for two terminal phosphorothioate linkages) has also been reported to have a high biological stability due to its tertiary structure (*33*) and is currently being tested as an anti-HIV agent (*34*).

## DISCUSSION

We have studied the protein binding characteristics and cell growth inhibitory effects of G-rich oligonucleotides that are backbone-modified analogues of the antiproliferative oligonucleotide, GRO29A. Previous work has identified the protein binding ability of GRO29A (*14*), and more recently, it was shown that this oligonucleotide can arrest the cells in the S-phase and inhibit DNA replication (*15*). The results of the present studies show that some, but not all, of the modified analogue oligonucleotides have strong antiproliferative effects against several cancer cell types. It is likely that these effects are not due to any antisense or antigene activity but rather are related to their specific secondary structure and its recognition by cellular proteins.

Previous reports have indicated that the nonantisense effects of G-rich oligonucleotides are related to their secondary structure (G-quartets) and protein binding (*35*, *36*). By employing UV and CD spectroscopy, we have detected a characteristic melting curve, indicating G-quartet formation by all modified GRO29A analogues tested. To our knowledge, this is the first report of full 2′-*O*-methyl RNA and mixed 2′-*O*-methyl RNA:DNA sequences being able to form

G-quartets. Interestingly, a recent paper showed that mRNA sequences involved in synaptic function or dendritic growth are capable of forming G-quartets. Moreover, these sequences were specifically targeted by the FMRP, a protein absent in the fragile X syndrome (*37*). This suggests a possible in vivo role for G-quartet formation by RNA sequences.

However, the presence of G-quartet formation was not sufficient for antiproliferative activity, since MR29A, which forms G-quartets, had no significant activity. Significant growth inhibitory activity was only observed for those G-quartet-forming oligonucleotides that could also compete for binding to a specific cellular protein(s) in a mobility shift assay. This supports our hypothesis that antiproliferative activity is mediated by binding to the protein.

Sequences containing G-quartets have been shown to bind to numerous cellular proteins (*5*, *14*, *38*−*40*). This relationship could be a part of transcriptional regulation, a general regulation of gene expression, telomere maintenance, and cell growth regulation. The proposed interaction site between GRO29A and the cellular protein(s) involves the core G-quartet region of the dimeric oligonucleotide structure. This is based on the structure−activity relationship we have developed with a number of substitutions in the G-quartet and loop regions. Therefore, a change in the structure of the G-quartet region should significantly alter the protein binding and antiproliferative activity. This is a possible explanation for the inability of MR29A to compete for protein and inhibit cell growth. Molecular modeling studies of GRO29A, MR29A, and MRdG29A demonstrated that the G-quartet regions are similar with respect to helical twist, rise, and sugar and phosphate backbone conformation, while the nature of the groove changes considerably depending on backbone type (Figure 5). These results indicate that oligonucleotide−protein interaction is highly selective and sensitive to change. Although, in this report, we did not specifically identify the protein which interacts with the oligonucleotides, there is evidence from our previous work that this protein is nucleolin (*14*). Nucleolin has previously been reported to bind to G-quartet sequences from telomeres (*41*), IgG switch regions (*5*, *42*) and ribosomal genes (*40*, *43*), as well as GRO29A (*14*), but its function as a G-quartet binding protein is not yet understood. The mechanism by which GRO29A binding to nucleolin can inhibit cell growth is still under investigation. The results presented in this report, however, confirm the importance of the specific G-rich oligonucleotide binding protein in the growth inhibitory properties of these oligonucleotides.

Our studies have also suggested that phosphodiester oligonucleotides may be the most useful backbone type for the development of therapeutic agents based on GRO29A. Although not generally considered to be suitable for in vivo use, due to their rapid degradation in serum, the stability of phosphodiester analogue of 29A is dramatically increased relative to that of non-G-quartet-forming oligonucleotides. This most likely reflects the very compact structure, which is assumed by these oligonucleotides, which is further stabilized by G-quartet formation.

Phosphorothioate oligonucleotides have been extensively tested in vivo and represent an alternative to phosphodiester ODNs. Even though PS29A has a similar efficacy compared to GRO29A, the phosphodiester molecule may have significant advantages over the phosphorothioate due to an expected decrease in nonspecific toxic side effects. The side effects seen with phosphorothioate oligonucleotides are most likely due to their polyanionic nature and their ability to stimulate the immune system (*17*). These toxicities are expected to be significantly reduced for phosphodiester oligonucleotides. The activity of the control phosphorothioate PS15B demonstrates that the mechanism of phosphorothioate effects may be very different (and less specific) from that of GRO29A.

Although full substitution of GRO29A with a 2′-*O*-methyl RNA backbone type abrogates antiproliferative activity, substitution of dT bases with 2′-*O*-methyluridine does not significantly reduce activity. Therefore, the mixed backbone oligonucleotide MRdG29A may also represent a promising molecule for therapeutic development.

While the exact mechanism of action of GRO29A and its analogues is still being investigated, it is likely that their growth inhibitory activity is related to their ability to bind one or more cellular proteins. It is clear that the ability of these oligonucleotides to form G-quartets and to bind to the cellular protein is related to their profound effects on cancer cell proliferation. It is important to stress that both of these characteristics are necessary for their activity but neither is sufficient by itself.

## REFERENCES


1. Galderisi, U., Di Bernardo, G., Melone, M. A., Galano, G., Cascino, A., Giordano, A., and Cipollaro, M. (1999) *J. Cell. Biochem. 74*, 31−37.
2. Helene, C., Giovannangeli, C., Guieysse-Peugeot, A. L., and Praseuth, D. (1997) *CIBA Found. Symp. 209*, 94−102.
3. Burgess, T. L., Fisher, E. F., Ross, S. L., Bready, J. V., Qian, Y. X., Bayewitch, L. A., Cohen, A. M., Herrera, C. J., Hu, S. S., Kramer, T. B., et al. (1995) *Proc. Natl. Acad. Sci. U.S.A. 92*, 4051−4055.
4. Williamson, J. R. (1994) *Annu. Rev. Biophys. Biomol. Struct. 23*, 703−730.
5. Dempsey, L. A., Sun, H., Hanakahi, L. A., and Maizels, N. (1999) *J. Biol. Chem. 274*, 1066−1071.
6. Kettani, A., Kumar, R. A., and Patel, D. J. (1995) *J. Mol. Biol. 254*, 638−656.
7. Simonsson, T., Pecinka, P., and Kubista, M. (1998) *Nucleic Acids Res. 26*, 1167−1172.
8. Catasti, P., Chen, X., Moyzis, R. K., Bradbury, E. M., and Gupta, G. (1996) *J. Mol. Biol. 264*, 534−545.
9. Sun, D., Thompson, B., Cathers, B. E., Salazar, M., Kerwin, S. M., Trent, J. O., Jenkins, T. C., Neidle, S., and Hurley, L. H. (1997) *J. Med. Chem. 40*, 2113−2116.
10. Haq, I., Trent, J., Chowdhry, B., and Jenkins, T. (1999) *J. Am. Chem. Soc. 121*, 1768−1779.
11. Newbold, R. F. (1999) *Anticancer Drug Des. 14*, 349−354.
12. Lavelle, F., Riou, J. F., Laoui, A., and Mailliet, P. (2000) *Crit. Rev. Oncol. Hematol. 34*, 111−126.
13. Meeker, A. K., and Coffey, D. S. (1997) *Biochemistry (Moscow) 62*, 1323−1331.
14. Bates, P. J., Kahlon, J. B., Thomas, S. D., Trent, J. O., and Miller, D. M. (1999) *J. Biol. Chem. 274*, 26369−26377.
15. Xu, X., Hamhouyia, F., Thomas, S. D., Burke, T. J., Girvan, A. C., McGregor, W. G., Trent, J. O., Miller, D. M., and Bates, P. J. (2001) *J. Biol. Chem. 276*, 43221−43230.
16. Agrawal, S., and Crooke, S. T. (1998) *Antisense research and application*, Springer, Berlin and New York.
17. Agrawal, S. (1999) *Biochim. Biophys. Acta 1489*, 53−68.
18. Crooke, S. T. (1999) *Biochim. Biophys. Acta 1489*, 31−44.
19. Eckstein, F. (2000) *Antisense Nucleic Acid Drug Dev. 10*, 117−121.
20. Waters, J. S., Webb, A., Cunningham, D., Clarke, P. A., Raynaud, F., di Stefano, F., and Cotter, F. E. (2000) *J. Clin. Oncol. 18*, 1812−1823.

21. Yuen, A. R., Halsey, J., Fisher, G. A., Holmlund, J. T., Geary, R. S., Kwoh, T. J., Dorr, A., and Sikic, B. I. (1999) *Clin. Cancer Res. 5*, 3357−3363.
22. Cunningham, C., Holmlund, J., Schiller, J., Geary, R., Kwoh, T., Dorr, A., and Nemunaitis, J. (2000) *Clin. Cancer Res. 6*, 1626−1631.
23. Nemunaitis, J., Holmlund, J. T., Kraynak, M., Richards, D., Bruce, J., Ognoskie, N., Kwoh, T. J., Geary, R., Dorr, A., Von Hoff, D., and Eckhardt, S. G. (1999) *J. Clin. Oncol. 17*, 3586−3595.
24. Morgan, D. M. (1998) *Methods Mol. Biol. 79*, 179−183.
25. Ausubel, F. M. (1994) *Current protocols in molecular biology*, John Wiley & Sons, New York.
26. Wang, Y., and Patel, D. J. (1993) *Structure 1*, 263−282.
27. Mohamadi, F., Richards, N. G., Cuida, W. C., Liskamp, R., Lipton, M., Caufield, C., Chang, G., Hendricksen, T., and Still, W. C. (1990) *J. Comput. Chem. 11*, 440.
28. Nicholls, A., Sharp, K. A., and Honig, B. (1991) *Proteins 11*, 281−296.
29. Gao, D., and Trent, J. O. (2001) GrooveView: A computer program for quantitating groove shapes in multistranded DNA complexes.
30. Mergny, J. L., Phan, A. T., and Lacroix, L. (1998) *FEBS Lett. 435*, 74−78.
31. Giraldo, R., Suzuki, M., Chapman, L., and Rhodes, D. (1994) *Proc. Natl. Acad. Sci. U.S.A. 91*, 7658−7662.
32. Jing, N., Rando, R. F., Pommier, Y., and Hogan, M. E. (1997) *Biochemistry 36*, 12498−12505.
33. Bishop, J. S., Guy-Caffey, J. K., Ojwang, J. O., Smith, S. R., Hogan, M. E., Cossum, P. A., Rando, R. F., and Chaudhary, N. (1996) *J. Biol. Chem. 271*, 5698−5703.
34. Este, J. A., Cabrera, C., Schols, D., Cherepanov, P., Gutierrez, A., Witvrouw, M., Pannecouque, C., Debyser, Z., Rando, R. F., Clotet, B., Desmyter, J., and De Clercq, E. (1998) *Mol. Pharmacol. 53*, 340−345.
35. Marathias, V. M., and Bolton, P. H. (1999) *Biochemistry 38*, 4355−4364.
36. Cheng, A. J., Wang, J. C., and Van Dyke, M. W. (1998) *Antisense Nucleic Acid Drug Dev. 8*, 215−225.
37. Darnell, J. C., Jensen, K. B., Jin, P., Brown, V., Warren, S. T., and Darnell, R. B. (2001) *Cell 107*, 489−499.
38. Ramanathan, M., Lantz, M., MacGregor, R. D., Garovoy, M. R., and Hunt, C. A. (1994) *J. Biol. Chem. 269*, 24564−24574.
39. Bianchi, A., and de Lange, T. (1999) *J. Biol. Chem. 274*, 21223−21227.
40. Hanakahi, L. A., Sun, H., and Maizels, N. (1999) *J. Biol. Chem. 274*, 15908−15912.
41. Pollice, A., Zibella, M. P., Bilaud, T., Laroche, T., Pulitzer, J. F., and Gilson, E. (2000) *Biochem. Biophys. Res. Commun. 268*, 909−915.
42. Hanakahi, L. A., Dempsey, L. A., Li, M. J., and Maizels, N. (1997) *Proc. Natl. Acad. Sci. U.S.A. 94*, 3605−3610.
43. Ghisolfi, L., Joseph, G., Erard, M., Escoubas, J. M., Mathieu, C., and Amalric, F. (1990) *Mol. Biol. Rep. 14*, 113−114.

BI0119520

THE JOURNAL OF BIOLOGICAL CHEMISTRY
Vol. 276, No. 46, Issue of November 16, pp. 43221–43230, 2001
Printed in U.S.A.


# Inhibition of DNA Replication and Induction of S Phase Cell Cycle Arrest by G-rich Oligonucleotides*

Received for publication, May 16, 2001, and in revised form, September 6, 2001
Published, JBC Papers in Press, September 12, 2001, DOI 10.1074/jbc.M104446200

**Xiaohua Xu‡, Fofi Hamhouyia‡, Shelia D. Thomas‡, Tom J. Burke§, Allicia C. Girvan¶, W. Glenn McGregor‡§, John O. Trent‡‖, Donald M. Miller‡¶, and Paula J. Bates‡¶****

*From the Human Molecular Biology Group, James Graham Brown Cancer Center, Departments of ‡Medicine, §Pharmacology/Toxicology, ¶Biochemistry/Molecular Biology, and ‖Chemistry, University of Louisville, Louisville, Kentucky 40202*

**The discovery of G-rich oligonucleotides (GROs) that have non-antisense antiproliferative activity against a number of cancer cell lines has been recently described. This biological activity of GROs was found to be associated with their ability to form stable G-quartet-containing structures and their binding to a specific cellular protein, most likely nucleolin (Bates, P. J., Kahlon, J. B., Thomas, S. D., Trent, J. O., and Miller, D. M. (1999) *J. Biol. Chem.* 274, 26369–26377). In this report, we further investigate the novel mechanism of GRO activity by examining their effects on cell cycle progression and on nucleic acid and protein biosynthesis. Cell cycle analysis of several tumor cell lines showed that cells accumulate in S phase in response to treatment with an active GRO. Analysis of 5-bromodeoxyuridine incorporation by these cells indicated the absence of *de novo* DNA synthesis, suggesting an arrest of the cell cycle predominantly in S phase. At the same time point, RNA and protein synthesis were found to be ongoing, indicating that arrest of DNA replication is a primary event in GRO-mediated inhibition of proliferation. This specific blockade of DNA replication eventually resulted in altered cell morphology and induction of apoptosis. To characterize further GRO-mediated inhibition of DNA replication, we used an *in vitro* assay based on replication of SV40 DNA. GROs were found to be capable of inhibiting DNA replication in the *in vitro* assay, and this activity was correlated to their antiproliferative effects. Furthermore, the effect of GROs on DNA replication in this assay was related to their inhibition of SV40 large T antigen helicase activity. The data presented suggest that the antiproliferative activity of GROs is a direct result of their inhibition of DNA replication, which may result from modulation of a replicative helicase activity.**

Oligonucleotides can recognize both nucleic acids and proteins with a high degree of specificity. This is a major reason why they have been widely investigated as potential therapeutic agents for cancer, viral infections, and inflammatory diseases. Oligonucleotides can achieve target recognition by sequence-specific interactions with nucleic acids or proteins such as in the antisense, antigene, or decoy approaches (1–4). Alternatively, target recognition can be due to the specific three-dimensional structure of an oligonucleotide, as in the aptamer approach (5, 6). These aptameric oligonucleotides often contain secondary structure elements such as hairpins or G-quartets. The formation of G-quartet structures is also thought to contribute to non-antisense growth inhibitory effects of G-rich phosphodiester and phosphorothioate oligonucleotides (7–9).

Recently, we reported (9) on a novel class of phosphodiester G-rich oligonucleotides (GROs)[1] that could strongly inhibit the *in vitro* proliferation of tumor cells derived from prostate, breast, and cervical carcinomas. The antiproliferative GROs were able to form stable secondary structures consistent with G-quartet formation. It was determined that these GROs bound to a specific nuclear protein and, furthermore, that the growth inhibitory activity of the GROs was positively correlated with their ability to bind to this protein. The specific GRO-binding protein was captured using biotinylated GROs and was identified by polyclonal and monoclonal antibodies to nucleolin. Therefore, we concluded that these potentially therapeutic oligonucleotides worked by a novel mechanism that involved binding to nucleolin or a nucleolin-like protein. Our hypothesis was that binding of GROs causes inhibition of nucleolin function(s) that results in an arrest of proliferation.

Nucleolin is an abundant 110-kDa phosphoprotein, thought to be located predominantly in the nucleolus of proliferating cells. Levels of nucleolin are known to relate to the rate of cellular proliferation (10, 11), being elevated in rapidly dividing cells such as malignant cells. Therefore, nucleolin may be an attractive molecular target for cancer therapy. The remarkable multifunctionality of nucleolin and its role in cell growth and proliferation have been highlighted in recent reviews (12–14). The most studied aspects of nucleolin function are its roles in ribosome biogenesis, which include the control of rDNA transcription, pre-ribosome packaging, and organization of nucleolar chromatin (12, 15). It is also thought that nucleolin can act as a shuttle protein that transports viral and cellular proteins between the cytoplasm and nucleus/nucleolus of the cell (16–18). In addition, nucleolin has been implicated, directly or indirectly, in other roles including nuclear matrix structure (19), DNA replication (20), cytokinesis and nuclear division (21), and as a nucleic acid helicase (12, 22). There have been numerous reports describing the presence of nucleolin in the plasma membrane of cells (9, 23–28), suggesting a further

* This work was supported by the Department of Defense Prostate Cancer Initiative, the National Institutes of Health, and the Commonwealth of Kentucky Research Challenge Trust. The costs of publication of this article were defrayed in part by the payment of page charges. This article must therefore be hereby marked "*advertisement*" in accordance with 18 U.S.C. Section 1734 solely to indicate this fact.

** To whom correspondence should be addressed: 204B Baxter Bldg., 570 S. Preston St., Louisville, KY 40202. Tel: 502-852-2432; Fax: 502-852-2356; E-mail: paula.bates@louisville.edu.

[1] The abbreviations used are: GROs, G-rich oligonucleotides; BrU, 5-bromouridine; BrdUrd, 5-bromo-2′-deoxyuridine; DMEM, Dulbecco's modification of Eagle's medium; PBS, phosphate-buffered saline; FCS, fetal calf serum; MTT, 3-(4,5-dimethylthiazol-2-yl)-2,5-diphenyltetrazolium bromide; RPA, replication protein A; TUNEL, terminal transferase dUTP nick-end label; NS, nonspecific oligonucleotide.

function of nucleolin as a cell surface receptor. Clearly, inhibition of nucleolin function, which we propose is an effect of GRO binding, would likely result in inhibition of cell proliferation and/or cell death.

To elucidate further the mechanism of the GRO antiproliferative activity, we decided to study the effects of GROs on cellular processes, such as nucleic acid and protein synthesis, and cell cycle progression. We report our findings that GROs specifically inhibit DNA replication, and we discuss the implications of these results in terms of potential mechanisms for GRO activity.

## EXPERIMENTAL PROCEDURES

*Oligonucleotides*—Except where indicated, oligonucleotides had phosphodiester backbones and 3′-C-3 aminoalkyl modifications. They were purchased from Oligos Etc. (Wilsonville, OR) or synthesized on a Beckman 1000M synthesizer using 3′-C-3-amine CPG columns from Glen Research (Sterling, VA). Oligonucleotides were resuspended in water, precipitated with butan-1-ol, washed with 70% ethanol, dried and resuspended in sterile 10 mM Tris·HCl, pH 7.5, or phosphate-buffered saline (PBS). They were then sterilized by filtration through a 0.2-$\mu$m filter and diluted with sterile buffer to give stock solutions of 400 or 500 $\mu$M that were stored in aliquots at −20 °C. Each oligonucleotide was checked for integrity by 5′-radiolabeling followed by polyacrylamide gel electrophoresis. Sequences of oligonucleotides used were as follows: GRO29A, 5′-TTTGGTGGTGGTGGTTGTGGTGGTGGTGG; GRO15B, 5′-TTGGGGGGGGTGGGT; GRO15A, 5′-GTTGTTTGGGGT-GGT; GRO26A, 5′-GGTTGGGGTGGGTGGGGTGGGTGGGG; GRO26B, 5′-GGTGGTGGTGGTTGTGGTGGTGGTGG; and CRO, 5′-TTTCCTCC-TCCTCCTTCTCCTCCTCCTCC.

*Flow Cytometry Analysis of Cell Cycle*—For the experiments shown in Figs. 1 and 2*B*, cells were plated in Dulbecco's modified Eagle's medium (DMEM, Life Technologies, Inc.) supplemented with 10% (v/v) fetal calf serum (FCS, Life Technologies, Inc.) and 1% penicillin/streptomycin solution (Life Technologies, Inc.) at a density of $10^5$ cells per well in a 6-well plate. After incubation at 37 °C for 4 h to permit adherence, cells were treated by direct addition of oligonucleotide to the culture medium to give a final concentration of 10 $\mu$M. For MDA-MB-231 cells only, a second dose of oligonucleotide was added 24 h after the first. At 72 h after the first dose, cells were harvested by trypsinization, fixed, and stained with propidium iodide using the Cycle Test Plus kit (Becton Dickinson). Cells were then analyzed using a FACScan cytometer. The percentage of cells in $G_1/G_0$, S, and $G_2$/M were determined using the Modfit program or, in a few cases where Modfit was unable to assign these parameters, by integrating peak areas using the CellQuest program. For the experiments shown in Fig. 2*B*, cells were treated as above and harvested at the times shown and analyzed as described.

*Synchronization of Cells*—To synchronize by serum starvation, cells were plated in complete medium (DMEM, 10% FCS, 1% antibiotic) at a density of $5 \times 10^4$ per well in 6-well plates and incubated overnight. Cells were washed three times with sterile PBS, and the medium was replaced with DMEM with 0.1% (v/v) FCS. After incubation in low serum medium for 48 h, medium was replaced with complete medium, and GRO29A was added directly to the medium to give 10 $\mu$M final concentration. To synchronize cells in S phase, cells were incubated for 16 h in complete medium containing 1 $\mu$g/ml aphidicolin. Cells were released by washing three times with PBS and adding complete medium. GRO29A was then added directly to the medium to give a final concentration of 10 $\mu$M. For each method of synchronization, samples were prepared in parallel to be harvested for flow cytometric analysis before release or 24 h after addition of GRO29A. Analysis of cell cycle was carried out as described above.

*DNA Synthesis Assay*—Cells were plated at a density of $1.5 \times 10^5$ cells per well, in a 48-well plate. Cells were incubated for 16 h and then treated by direct addition of oligonucleotide to the culture medium at a final concentration of 12 $\mu$M (or untreated samples received an equal volume of sterile PBS). A second identical dose was given 60 h after the first. 72 h after the first treatment, cells were pulsed by addition of BrdUrd (Sigma, final concentration 10 $\mu$M) to the medium for 1 h at 37 °C. Cells were washed three times with PBS and fixed with methanol for 10 min at room temperature. Samples were washed with PBS, incubated with 2 M HCl (to denature DNA) for 10 min on ice, washed, and neutralized with 0.1 M sodium borate. The cells were then incubated with anti-BrdUrd monoclonal antibody (Becton Dickinson, used at 1.7 $\mu$g/ml) for 30 min at room temperature, washed, and incubated with Alexa488-labeled goat anti-mouse IgG (Molecular Probes, used at 4 $\mu$g/ml) for 20 min at room temperature. After washing, cells were viewed with a Nikon Eclipse TS100 microscope with ELWD epifluorescence attachment, and digital images were captured using a Olympus DP10 camera.

*RNA Synthesis Assay*—Samples shown in Fig. 4*B* were prepared exactly as described for DNA synthesis, and after 72 h of incubation with oligonucleotide samples were pulsed by addition of BrU (Aldrich) at a final concentration of 1 mM for 1 h at 37 °C. Cells were fixed with 4% (w/v) paraformaldehyde in PBS, stained as above (1.7 $\mu$g/ml anti-BrdUrd followed by 4 $\mu$g/ml Alexa488-labeled anti-mouse IgG), and photographed as described above. For the samples shown in Fig. 4*A*, cells were treated with 0.1 $\mu$g/ml actinomycin D for 1 h at 37 °C prior to pulsing with BrU or were incubated with 2.5 mg/ml RNase A for 30 min after fixing.

*Protein Synthesis Assay*—Samples were prepared exactly as described for DNA synthesis. After 72 h of incubation with oligonucleotide, cells were washed twice with methionine/cysteine-free medium (Life Technologies, Inc.), incubated for 15 min at 37 °C in this medium, and then pulsed by addition of [$^{35}$S]methionine (final concentration 40 $\mu$Ci/ml) for 1 h at 37 °C. After washing, proteins were extracted by addition of 100 $\mu$l of citrate saline solution and precipitated by addition of 400 $\mu$l of 10% trichloroacetic acid and 20 mM pyrophosphate. An aliquot of this solution was used to quantitate total protein using the BCA Protein Assay (Pierce), and the remainder was filtered through a glass filter to determine trichloroacetic acid-precipitable counts. Protein synthesis was expressed as counts/min per $\mu$g of total protein. Experiments were performed in triplicate, and error bars represent the S.E.

*TUNEL Staining and Cell Morphology*—Cells were plated ($1.5 \times 10^4$ cells per well for DU145 or $4 \times 10^4$ cells per well for MDA-MB-231) in 24-well plates containing glass coverslips (Fisher) that had been washed and sterilized. Oligonucleotide was added directly to the medium to a final concentration of 10 $\mu$M at 4 h after plating. Further identical doses were given at 24 and 72 h subsequent to the first dose (cells shown in Fig. 6*A* did not receive the third dose). At the appropriate time, cells were washed with PBS and fixed for 15 min at room temperature with 4% (w/v) paraformaldehyde in PBS. Cells were permeabilized by incubation in 0.1% Triton X-100, 0.1% sodium citrate for 2 min on ice. Terminal transferase-mediated labeling of fragmented DNA with dUTP was carried out using *In Situ* Cell Death Detection kit (Roche Molecular Biochemicals), according to the manufacturer's instructions. For morphology analysis cells were prepared as above and viewed using an Olympus BX60 microscope.

*SV40 DNA Replication Assay*—Replication-competent cell extracts were prepared from HeLa cells by a modification of the method of Li and Kelly (29, 30). HeLa cells were grown in DMEM (Life Technologies, Inc.) with 10% supplemented calf serum (HyClone) and antibiotics and were maintained in logarithmic growth. Briefly, the cells were released, combined, and washed once with isotonic buffer (20 mM HEPES, 5 mM KCl, 1.5 mM $MgCl_2$, 1 mM dithiothreitol, 250 mM sucrose) and twice with hypotonic buffer (isotonic buffer without sucrose). Following the second hypotonic wash, the cell count was adjusted to $7 \times 10^7$ cells/ml, and the suspension was placed on ice for 30 min. The cells were gently lysed using a Dounce glass homogenizer and a tight-fitting plunger and then placed on ice for 30 min. The suspension was centrifuged at 10,000 rpm for 10 min at 4 °C, and the supernatant was frozen by dripping it through liquid nitrogen. Replication reactions were carried out using the M13mp2SV replication template (7406 base pairs), which is an M13mp2 molecule containing the SV40 origin of replication (31). Replicative form templates were prepared from infected *recA Escherichia coli* by standard methods, and covalently closed circular (form I) DNA was isolated by two successive CsCl gradients. Template (40 ng) was preincubated with water or the oligonucleotide (400 nM final concentration) as indicated for 30 min at 37 °C and then added to reaction mixes as described previously (32). Replication reactions (25 $\mu$l) contained 30 mM HEPES, pH 7.8, 7 mM $MgCl_2$, 4 mM ATP, 200 $\mu$M each of CTP, GTP, and UTP, 100 $\mu$M each of dATP, dGTP, dCTP, TTP, and [$\alpha$-$^{32}$P]dCTP (6,600 dpm/fmol), 40 mM creatine phosphate, 2 $\mu$g of creatine kinase, and 15 mM sodium phosphate, pH 7.5. The SV40 large T antigen (Molecular Biology Resources) was omitted from the negative control (Fig. 7, *1st lane*), and 1 $\mu$g was added to all other tubes. After addition of cell extract (75 $\mu$g of protein) to each tube, the reactions proceeded for 2 h at 37 °C. At this time, an equal volume of stop solution (2% SDS, 50 mM EDTA, 2 mg/ml proteinase K) was added, and the samples were incubated for an additional 30 min at 37 °C. An aliquot (1/10 volume) was taken for determination of [$\alpha$-$^{32}$P]dCTP into acid-insoluble material, and picomoles of dCTP incorporated was calculated. The relative dCTP incorporation stated in the text represents the average of three

independent experiments, and standard errors of the data are shown. The DNA was extracted, and aliquots were electrophoresed on 1% (w/v) agarose gels containing 0.5 μg/ml ethidium bromide. The dried gels were imaged on a Storm PhosphorImager (Molecular Dynamics), and the density of the bands corresponding to covalently closed circular (form I) DNA was quantified using ImageQuant software.

*Cell Proliferation Assay*—HeLa cells were plated at $10^3$ cells per well in 96-well plates. After incubation for 16 h, oligonucleotide was added directly to the culture medium to give a final concentration of 12 μM. Culture medium was not changed throughout the duration of the experiment. The relative number of viable cells in each well was determined 96 h after addition of oligonucleotides using the MTT assay (33). Briefly, 15 μl of 5 mg/ml 3-(4,5-dimethylthiazol-2-yl)2,5-diphenyltetrazolium bromide (MTT, Sigma) was added to each well. Following 16 h of incubation at 37 °C, cells were lysed by addition of 75 μl per well of 10% SDS, 10 mM HCl, and after a further 16 h of incubation at 37 °C, absorbance at 570 nm was determined using a Molecular Devices microplate reader. Experiments were performed in triplicate, and bars represent the S.E.

*Helicase Assay*—These assays were carried out according to a method similar to that of Veaute *et al.* (34). Oligonucleotide 55A (5′-TGAAGGTTTCGAATCAGAGGTAGGTGCCCGGCCTCCAACTTGCCGTATTCCTGGT, unmodified phosphodiester, purchased from Life Technologies, Inc.) was 5′-labeled using T4 kinase and [γ-$^{32}$P]ATP. After removal of unincorporated [$^{32}$P]ATP it was annealed (95 °C for 5 min followed by slow cooling to room temperature) to a partially complementary oligonucleotide 55B (5′-ACCAGGAATACGGCAAGTTGGAGGCCGGGCTGGATGGAGACTAAGCTTTGGAAGT, unmodified phosphodiester, purchased from Life Technologies, Inc.) in order to form the synthetic replication fork substrate containing a region of 30 base pairs (underlined). Unwinding of this substrate by recombinant SV40 large T antigen (Chimerx, Milwaukee, WI) was carried out by incubating 10 fmol of substrate with 100 ng of large T antigen in the absence or presence of competitor unlabeled oligonucleotides in a final volume of 10 μl of HA buffer (20 mM Tris·HCl, pH 7.5, 7 mM $MgCl_2$, 5 mM dithiothreitol, 2 mM ATP, and 25 μg/ml bovine serum albumin). Large T antigen was preincubated for 15 min at 37 °C prior to addition. The reaction was allowed to proceed for 15 min at 37 °C before being terminated by addition of STOP buffer (200 mM EDTA, 40% glycerol, 0.6% SDS, 0.15% bromphenol blue, 0.15% xylene cyanol). Samples were analyzed by native polyacrylamide electrophoresis on 8% polyacrylamide gels containing 1× TBE (90 mM Tris borate, pH 8.3, 2 mM EDTA) with 1× TBE, 0.1% SDS as running buffer. For the assay shown in Fig. 8*A*, the nonspecific competitor oligonucleotide was (NS) (5′-AGGACTGTATACTGTCTTGGA, unmodified phosphodiester, purchased from Life Technologies, Inc.), and 29A is this assay was also unmodified. For the assay shown in Fig. 8*B*, all oligonucleotides except NS were modified with a 3′-C-3 aminoalkyl group.

*Nucleolin-Replication Protein A (RPA) Interaction*—Immunoprecipitation was carried out in 0.5 ml of RIPA buffer (50 mM Tris·HCl, pH 7.5, 0.5 M NaCl, 0.1 mM EDTA, 100 μM NaF, 1 mM $Na_3VO_4$, 1% Nonidet P-40, 0.5% sodium deoxycholate, 0.1% SDS, 1 mM phenylmethylsulfonyl fluoride, 1 μM leupeptin, 10 μM aprotinin) for 30 min at 37 °C using 25 μg of HeLa extracts (as used for *in vitro* replication) and 5 μg of monoclonal antibody to 14-kDa subunit of RPA (Novus Biologicals). Antibodies were captured for 1 h at 4 °C using magnetic beads linked to goat anti-mouse IgG (Magnabind, Pierce), washed three times with 0.5 ml of RIPA, and eluted by heating the beads for 15 min at 65 °C in a buffer containing 2% SDS and 5% 2-mercaptoethanol. To investigate the effect of GROs on nucleolin-RPA interaction, the HeLa extracts were preincubated for 30 min at 37 °C in the absence or presence of oligonucleotides. Precipitated proteins were electrophoresed on 8% polyacrylamide/SDS gels, transferred to polyvinylidene difluoride membrane, Western-blotted using nucleolin monoclonal antibody (Santa Cruz Biotechnology, 1:200 dilution) and peroxidase-linked goat anti-mouse (Santa Cruz Biotechnology, 1:1000), and visualized by chemiluminescence.

## RESULTS

*Accumulation of GRO29A-treated Cells in S Phase*—To investigate cell cycle perturbations induced by antiproliferative G-rich oligonucleotides, flow cytometry analysis of propidium iodide stained nuclei was performed. Cell cycle parameters were compared for untreated cells and cells that had been treated for 72 h with an active GRO (GRO29A) or a control inactive GRO (GRO15B). The cell lines examined were DU145 (derived from prostate carcinoma), MDA-MB-231 (breast carcinoma), HeLa (cervical carcinoma), and HS27 (normal foreskin fibroblasts). In all of the carcinoma lines, we observed a significant increase in the fraction of cells in the S phase of the cell cycle for cells treated with GRO29A, as shown in Fig. 1. This was accompanied by a decrease in the proportion of cells in the $G_0/G_1$ and $G_2/M$ phases of the cell cycle, as indicated in Fig. 1. These changes were specific for GRO29A and not simply due to the presence of oligonucleotide, because cells treated with GRO15B were similar to untreated cells.

We also observed the appearance of a peak corresponding to a population of cells with sub-$G_1$ DNA content (marked with an *asterisk* in Fig. 1). This peak, which is indicative of apoptotic cells, appeared in the tumor cell samples treated with GRO29A but was much smaller in the GRO15B-treated or untreated cells. The induction of apoptosis by GRO29A was examined further and will be described below.

In contrast to the malignant cell lines, HS27 cells, which are derived from normal skin fibroblasts, showed no major perturbations in cell cycle in response to treatment with GRO29A. The HS27 cells were also found to be considerably less sensitive to the antiproliferative effects of GRO29A than most of the tumor cell lines we have examined.[2] However, it can be seen from the data (Fig. 1, *untreated*) that the HS27 cells have a much lower proportion in S phase (even though they are subconfluent), compared with the tumor cell lines, and proliferate at a slower rate. To test whether the response of cells is related to the proportion of cells in S phase when GRO is added, we partially synchronized DU145 cells and added GRO29A when the cells were predominantly in S phase (after aphidicolin treatment) or $G_1/G_0$ (after serum starvation). Fig. 2*A* shows that the cells showed similar S phase accumulation, irrespective of the proportion of cells in S phase when GRO was added. These data suggest that the differential responsiveness of HS27 cells is not necessarily related to the lower proportion of these cells in S phase, but further studies are required to confirm the tumor selectivity of GRO29A and investigate the mechanism of selectivity.

Studies of cell cycle progression following partial synchronization of tumor cells showed that even when GRO29A was added in $G_1/G_0$ (following serum synchronization) or early S phase (following aphidicolin treatment), a considerable proportion of the cells were able to progress through S phase and $G_2/M$ (data not shown). In fact, the accumulation of cells in S phase was found to be a gradual process that occurs over several cell cycles, as shown in Fig. 2*B* for unsynchronized DU145 cells treated with GRO29A. The gradual arrest of cells in S phase may be related to the rate of oligonucleotide uptake, which is thought to be relatively slow. We are currently investigating the relationship between GRO uptake and cell cycle arrest.

*Inhibition of DNA Replication in Cells*—The S phase of the cell division cycle represents the period in which cells replicate their DNA (and thus have a DNA content intermediate between that of $G_0/G_1$ and $G_2/M$ cells). In this case, because cell proliferation is inhibited by GRO29A, it seems unlikely that the increase in the S phase fraction represents an increase in cells that are actively replicating DNA but more likely an accumulation of cells whose progress is arrested in this phase of the cell cycle.

To confirm this hypothesis, we analyzed DNA replication in cells treated with GROs. This was achieved by determining incorporation of 5-bromo-2′-deoxyuridine (BrdUrd), a nucleo-

[2] P. J. Bates, S. D. Thomas, J. O. Trent, and D. M. Miller, unpublished observations.

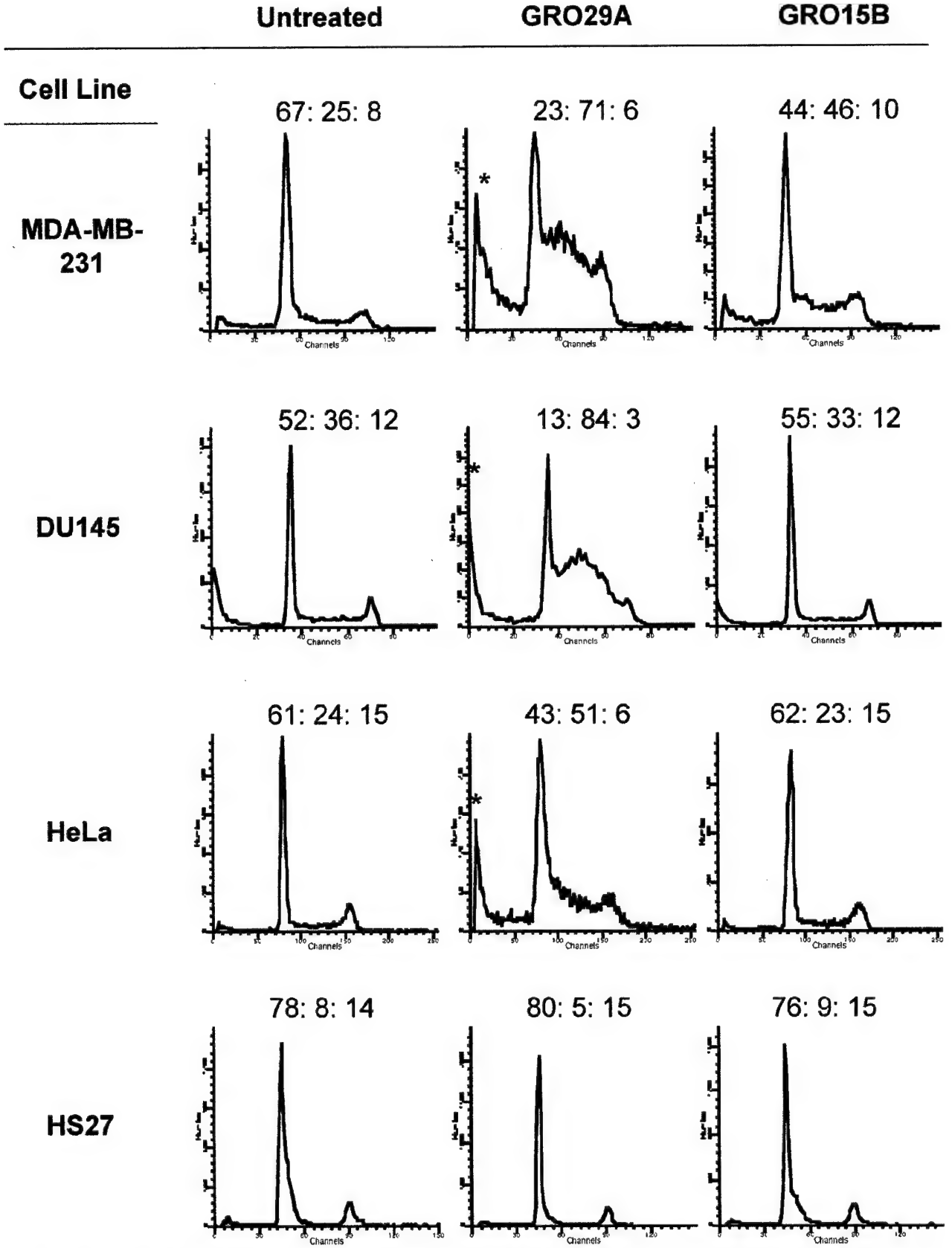


FIG. 1. **Flow cytometric analysis of cell cycle parameters following 72 h of treatment with active GRO29A or inactive control GRO15B, compared with untreated cells.** The identity of the cell line is indicated on the *left*, and *numbers above* each histogram indicate the ratio of cells in the $G_1/G_0$, S, and $G_2/M$ phases of the cell cycle (data were gated to exclude apoptotic cells for these calculations). The *peak* marked by an *asterisk* represents apoptotic cells with sub-$G_1$ DNA content.

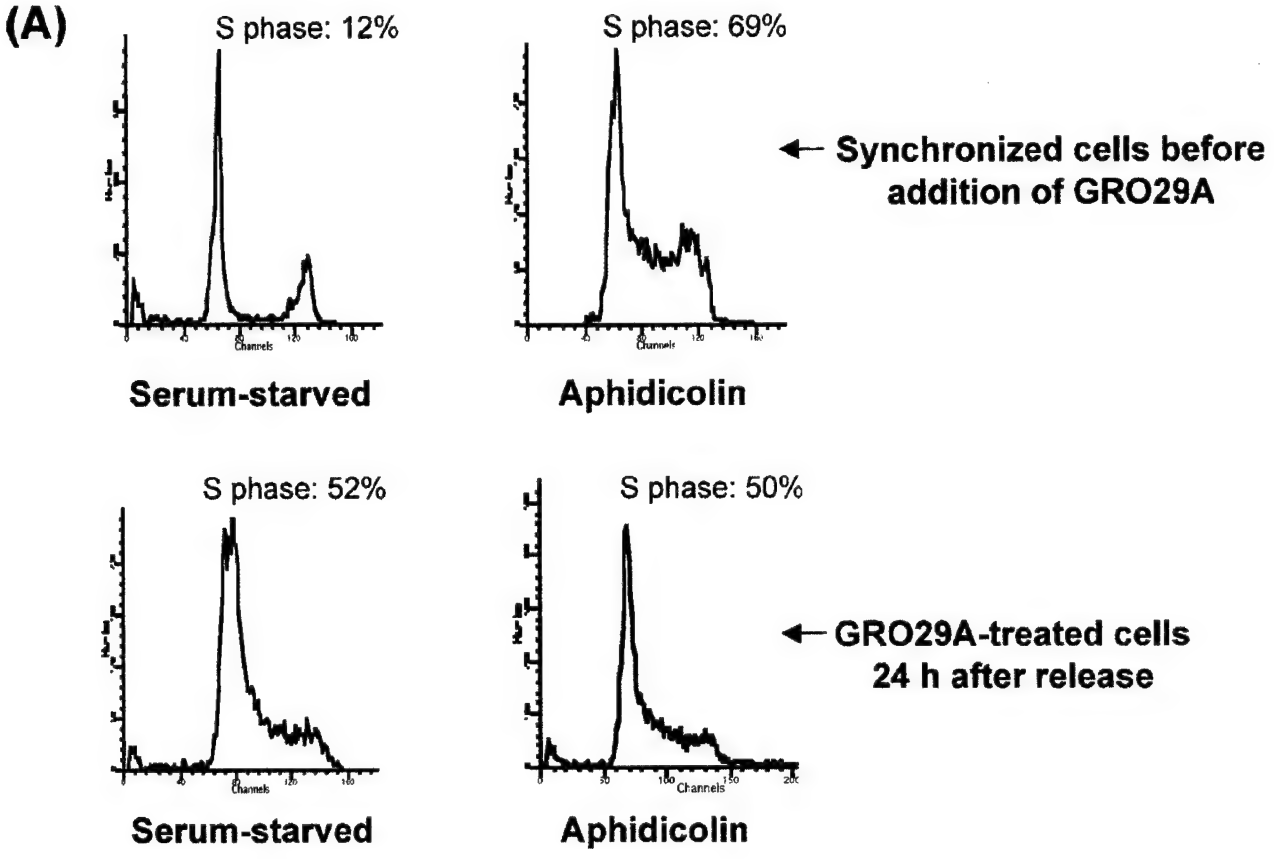


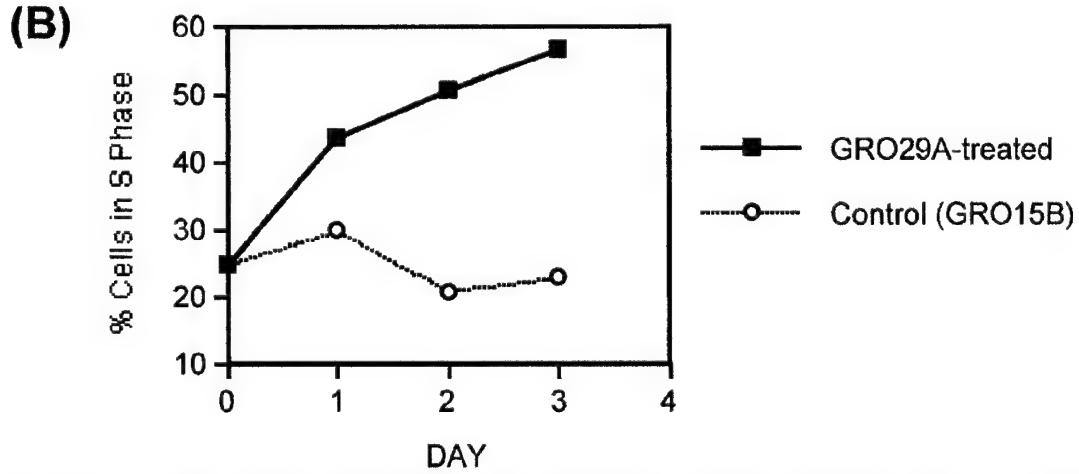


FIG. 2. *A*, flow cytometric analysis of cell cycle parameters. DU145 cells were partially synchronized by either serum starvation or aphidicolin treatment (*top panel*). Cells were treated with 10 μM GRO29A at the time of release from synchronization and analyzed after 24 h (*bottom panel*). *B*, graph showing the percentage of cells accumulated in S phase for asynchronous DU145 cells treated with GRO29A or control oligonucleotide (GRO15B).

side that can be incorporated into cellular DNA in place of thymidine. A BrdUrd antibody can then positively stain cells that actively synthesize DNA during the BrdUrd pulse. In this experiment. DU145 cells were incubated as described in the absence or presence of GROs for 72 h, at which time BrdUrd was added to the cell culture medium for 1 h. Cells were then fixed with methanol, and incorporation of BrdUrd was assessed by indirect immunofluorescent staining using a BrdUrd antibody. Fig. 3 shows the results of these experiments. In the untreated sample. ~40% of cells was found to be positive for BrdUrd staining. However, the cells treated with GRO29A showed an almost complete absence of staining. indicating that no *de novo* DNA synthesis was occurring in these cells. This effect was specific for GRO29A, because cells treated with the control oligonucleotide (GRO15B) had similar BrdUrd incorporation to untreated cells.

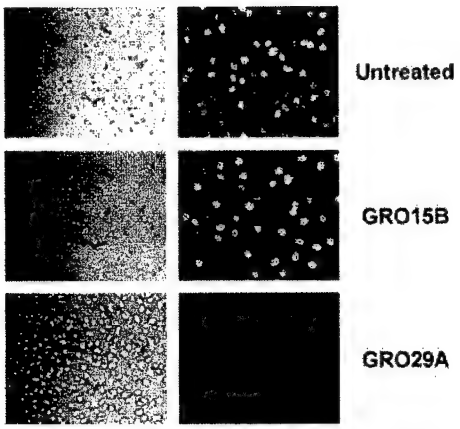


FIG. 3. **DNA synthesis in untreated DU145 cells and cells treated with GRO15B (control oligonucleotide) or GRO29A (active oligonucleotide).** Cells were treated for 72 h and then pulsed with BrdUrd. Incorporation of BrdUrd was detected by indirect immunofluorescence using a BrdUrd monoclonal antibody.

To confirm that the effects of GRO29A on cell cycle and DNA synthesis occur in parallel, we carried out one further experiment. DU145 cells were treated in a 6-well plate, pulsed with BrdUrd for 1 h, then collected by trypsinization, and divided into 2 aliquots. One aliquot was stained with propidium iodide and analyzed by flow cytometry, and the other aliquot was used to prepare slides for staining with BrdUrd antibody. The results indicated that for the same sample of GRO29A-treated cells, there was an accumulation in S phase concurrent with an inhibition of DNA synthesis (data not shown).

The time course of inhibition of DNA replication depended on a number of factors, including the initial cell density and the number and schedule of GRO29A doses. When DU145 cells were plated at $6.25 \times 10^3$ cells per well in a 24-well plate, and treated after 17 h with 10 $\mu$M final concentration of GRO, we found no significant difference between DNA synthesis in treated and untreated cells at 3, 6, and 9 h after addition of GRO29A. However, at 12 h after treatment, only 28% of cells stained positive for BrdUrd in the GRO29A-treated sample, compared with 41 and 44%, respectively, in the untreated and GRO15B treated cells. By 24 h after addition of oligonucleotide, the GRO29A-treated cells were completely negative for BrdUrd staining.

*Effect of GROs on RNA and Protein Synthesis*—Because inhibition of any one of DNA, RNA, or protein synthesis is expected to lead eventually to inhibition of the other processes, it is important to determine which of these functions is arrested first. To investigate this, we examined both RNA and protein synthesis in parallel with DNA replication, at a time point at which DNA synthesis was known to be completely inhibited. As described above, DNA replication was assessed by BrdUrd incorporation, and a similar method was used to determine RNA synthesis. This method has been described previously (35, 36) and involves detection of incorporated 5-bromouridine (BrU) by indirect immunofluorescent staining with a BrdUrd antibody (which is cross-reactive for BrU). To ensure that the BrU staining represents *bona fide* RNA synthesis, we carried out a preliminary experiment to assess the effects of treatment with RNase or actinomycin D, an inhibitor of RNA synthesis. Fig. 4*A* shows that staining in these samples was negative, indicating that this technique accurately reflects RNA synthesis.

Fig. 4*B* shows the effects of GRO treatment on RNA synthesis in DU145 cells. After incubation for 72 h in the absence or presence of GROs, cells treated with GRO29A showed staining

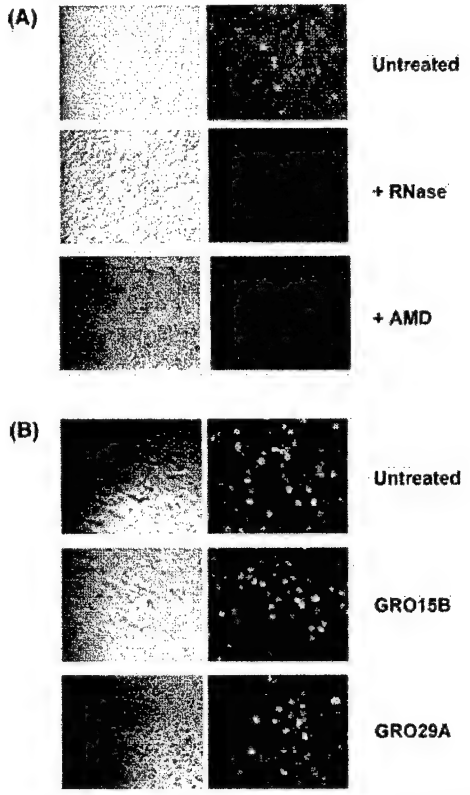


FIG. 4. *A*, DU145 cells were treated with RNase A or actinomycin D (an RNA synthesis inhibitor) and compared with untreated cells to demonstrate that the staining procedure for RNA synthesis was specific. Cells were pulsed with BrU, and incorporation of BrU was detected by indirect immunofluorescence using a cross-reactive BrdUrd monoclonal antibody. *B*, RNA synthesis in untreated DU145 cells and cells treated with GRO15B (control oligonucleotide) or GRO29A (active oligonucleotide). Cells were treated for 72 h and then pulsed with BrU and stained as described.

for BrU incorporation similar to that for untreated and control (GRO15B)-treated samples. Cells that had been treated in parallel and pulsed with BrdUrd demonstrated negative staining for DNA synthesis in the GRO29A-treated sample (shown in Fig. 3). Therefore, it appears that RNA synthesis is still occurring in GRO29A-treated cells at a time when DNA synthesis is arrested.

To determine global protein synthesis, the incorporation of [$^{35}$S]methionine was examined. Cells were incubated for 72 h in the absence or presence of GROs and pulsed with [$^{35}$S]methionine, and radioactivity associated with trichloroacetic acid-precipitable material was determined by scintillation counting. To normalize the data for differences in the number of cells, the total protein content for each sample was determined by the Bradford assay, and protein synthesis was expressed as counts per $\mu$g of total protein. Parallel samples were pulsed with BrdUrd in place of [$^{35}$S]methionine to monitor DNA synthesis. Fig. 5 shows that there was no significant difference in the levels of global protein synthesis between untreated cells and cells treated with GRO29A or GRO15B, whereas DNA synthesis was completely inhibited by GRO29A (Fig. 3).

*Induction of Apoptosis and Changes in Cell Morphology*—Induction of apoptosis by GRO29A was suggested by the appearance of cells with sub-$G_1$ DNA content in the flow cytometry cell cycle analysis (Fig. 1). We confirmed this finding by carrying out terminal transferase dUTP nick-end label (TUNEL) staining of GRO-treated cells. Fig. 6*A* shows that there was minimal TUNEL staining in untreated DU145 cells

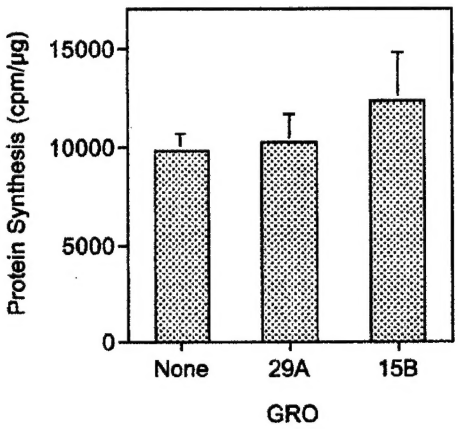


FIG. 5. **Protein synthesis in untreated DU145 cells and cells treated with GRO15B (control oligonucleotide) or GRO29A (active oligonucleotide).** Cells were treated for 72 h, transferred to methionine/cysteine-free medium, and then pulsed with $^{35}$S-labeled methionine. Protein synthesis was determined by scintillation counting of trichloroacetic acid-precipitable material and was normalized by determining the total protein content of the sample and expressing as counts/min per μg of total protein.

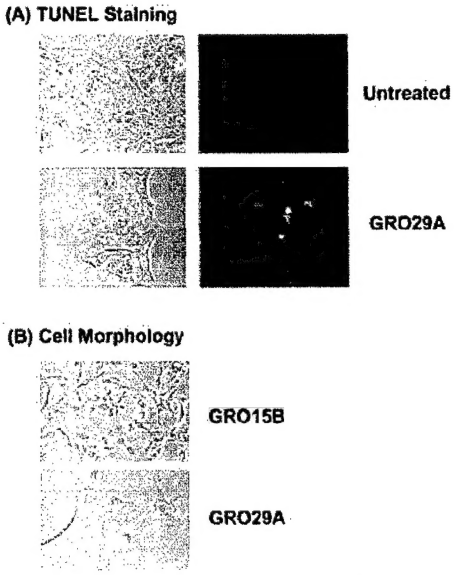


FIG. 6. *A*, TUNEL staining to show induction of apoptosis in DU145 prostate cancer cells by GRO29A. Cells were treated for 72 h and stained as described. Cells treated with GRO15B (not shown) had similar staining to the untreated samples. *B*, phase contrast micrographs of MDA-MB-231 breast cancer cells to show differences in morphology induced by treatment with an active GRO (29A) compared with the control GRO (15B).

(and in control 15B-treated samples, not shown). The sample treated with GRO29A showed a punctate pattern of positive nucleoplasmic and perinuclear staining, consistent with end labeling of fragmented DNA, an indicator of apoptosis. Although some of the treated cells had the classic features of apoptosis, at longer treatment times some cells had morphology characterized by greatly enlarged nuclei and cytoplasm. As shown in Fig. 6*B*, this was particularly evident in MDA-MB-231 breast cancer cells that had been treated for 5 days with GRO29A. The significance of this proportion of enlarged cells is unclear at present but is consistent with our observation that protein synthesis is ongoing, whereas DNA replication and cell division are inhibited.

*Inhibition of DNA Replication in Vitro*—The data presented suggest that inhibition of DNA replication is a primary event associated with cell response to treatment with antiproliferative GRO. In cells, arrest of DNA synthesis can occur as a direct consequence of interference with the organization or progress of the DNA replication machinery. Alternatively, DNA replication could be arrested secondary to other effects, such as alterations in signaling pathways.

To elucidate further the mechanism of GRO29A-induced inhibition of DNA replication, we examined the effects of GROs on replication in an *in vitro* system (29, 30). This system utilizes HeLa cell extracts to replicate a plasmid containing the simian virus (SV40) origin of replication and requires addition of SV40 large T antigen, most probably to facilitate unwinding of the template (37, 38). By using this assay, 400 nM GRO29A was reproducibly found to inhibit DNA replication *in vitro* by about 90% (incorporation of dCTP was 9.1 ± 1.6% compared with control), whereas the same concentration of GRO15B had no effect (97.8 ± 7.1% dCTP incorporation compared with control). This assay was then used to examine a series of GROs with a variety of antiproliferative activities. These oligonucleotides have been described previously (9), with the exception of GRO26B, which is an active analog of GRO29A that lacks the three 5′-thymidines. Fig. 7*A* shows representative results from the *in vitro* replication assays. The relative inhibition is shown as a percentage of the control below the gel and was determined by integration of the bands representing the closed circular (form I) replication product. The ability of these same oligonucleotides to inhibit the proliferation of HeLa cells in culture is shown in Fig. 7*B*. Oligonucleotides 29A and 26B were found to strongly inhibit cell proliferation, 26A showed intermediate inhibitory activity, and 15A, 15B, and CRO had little or no activity. (Although we reported previously (9) some antiproliferative activity in HeLa cells for multiple doses of 15A, there was no activity when cells were treated with a single dose.) The relative activities of the six oligonucleotides in cells were almost identical to those observed in the SV40 replication assay. Therefore, we conclude that the ability of oligonucleotides to inhibit cellular proliferation is correlated with their ability to inhibit DNA replication and that this blockade of replication is due to a direct effect of GRO on the DNA replication machinery.

*Effect of GRO29A on RPA-Nucleolin Interaction and SV40 Large T Antigen Helicase Activity*—Inhibition of *in vitro* DNA replication by GRO29A most probably occurs because the G-rich oligonucleotide interferes with the assembly or progression of the complex that carries out the replication process. Many of the proteins that are required for efficient replication, both in the *in vitro* system and in cells, have now been identified (39–41). Based on the existing literature, we believe the most likely replication-associated proteins to be modulated GRO29A are replication protein A (RPA), which is known to bind to nucleolin (20), or the SV40 large T antigen, which can bind to G-quartet structures (42).

RPA is a single-stranded DNA-binding protein that plays a pivotal role in DNA replication, repair, and homologous recombination. It is possible RPA could bind directly to GRO29A, but simple single strand DNA binding would not explain the inability of other oligonucleotides (for example, 15B and CRO) to inhibit replication. There is also the possibility that GROs can modulate the interaction between RPA and nucleolin (the putative GRO-binding protein), which was recently reported by Daniely and Borowiec (20). These authors demonstrated that this interaction occurs *in vitro* and found that addition of exogenous nucleolin protein to the SV40 replication assay strongly reduced origin unwinding and DNA replication in this system. This was presumed to be a result of nucleolin binding to and inactivating RPA, because replication could be rescued

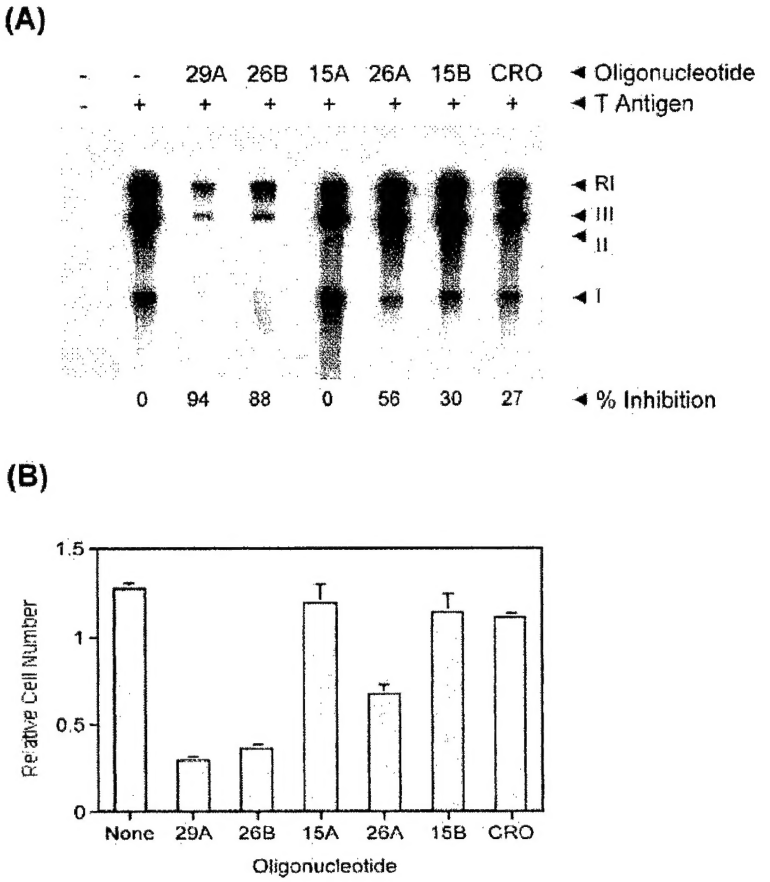


FIG. 7. *A*, effect of various oligonucleotides on the efficiency of DNA replication *in vitro*. The indicated oligonucleotide was mixed with the DNA template, and buffer and cell extracts were added. The reaction was started by the addition of SV40 large T antigen and proceeded for 2 h at 37 °C. The T antigen was omitted from the negative control (*far left lane*). The reaction was stopped after 2 h at 37 °C. The bands indicated represent covalently closed circular (*I*), nicked (*II*), and linear (*III*) forms of DNA, and *RI* indicates replication intermediates. The density of the form I was determined with ImageQuant software, and the data were used to calculate the percentage inhibition of replication compared with the positive control (no oligonucleotide added), which is shown *below* each lane. *B*, graph indicating the relative number of viable HeLa cells (as determined by the absorbance at 570 nm following MTT assay) 96 h after treatment with a single dose (12 $\mu$M) of the oligonucleotide indicated.

by addition of extra RPA. It was also reported that heat shock of HeLa cells caused a redistribution of nucleolin from the nucleoli to the nucleoplasm, and the authors (20) proposed that this redistribution and the resultant binding of nucleolin to RPA was a mechanism for repression of chromosomal replication in response to cell stress. If binding of nucleolin to GRO29A caused a conformational change that enhanced the affinity of nucleolin for RPA, this would explain the inhibition of replication both *in vitro* and in cells. To test this hypothesis, we carried out immunoprecipitation of HeLa cell extracts with an antibody to the 14-kDa subunit of RPA in the absence or presence of various GROs. In accord with Daniely and Borowiec (20), we could detect nucleolin in the immunoprecipitated proteins by Western blotting (data not shown). However, the presence of GROs at 100–1000 nM final concentration (which was sufficient to inhibit *in vitro* replication) did not significantly alter the amount of nucleolin precipitated with anti-RPA antibody. Treatment of HeLa cells with GRO29A also did not cause significant redistribution of nucleolin from the nucleoli to the nucleoplasm (as assessed by immunofluorescent microscopy, data not shown). Therefore, there is no evidence to support the hypothesis that the nucleolin-RPA interaction is modulated by GRO29A.

An alternative mechanism for the inhibition of DNA replication in the SV40 system is the inhibition of large T antigen helicase activity by GRO29A. The ability of T antigen to unwind structures containing G-quartets has been documented previously (42); therefore, we postulated that the presence of an excess of G-quartet containing oligonucleotide could sequester the helicase activity and prevent template unwinding and replication. To test this hypothesis we carried out T antigen helicase assays in the presence of various oligonucleotides. Because T antigen has a single-stranded DNA binding domain, it is important to demonstrate that any inhibition by oligonucleotides is specific. Therefore, we first compared inhibition of helicase activity by an active GRO (29A) and a nonspecific oligonucleotide (NS). Fig. 8*A* shows that GRO29A is significantly more active than NS at inhibiting helicase activity. To compare the relative ability of the oligonucleotides used in the replication assay to inhibit helicase activity, we carried out similar experiments with 50 nM final oligonucleotide concentration (at which there was a clear difference between GRO29A and NS). Fig. 8*B* shows the results of these experiments. Oligonucleotides 29A, 26B, and 26A were active in inhibiting unwinding by T antigen, whereas 15A, 15B, and CRO were not. The inactivity of CRO (which is the same length as 29A) shows that inhibition of helicase activity was not simply a function of oligonucleotide length. Comparison of the data in Fig. 8*B* with those shown in Fig. 7 indicates a good correlation between inhibition of helicase activity, inhibition of *in vitro* DNA replication, and inhibition of cell growth.

## DISCUSSION

GROs are a new type of antiproliferative oligonucleotide with considerable potential as therapeutic agents for cancer. Although the activity of GROs is known to correlate with their ability to bind to nucleolin protein, the precise mechanism by which they exert their antiproliferative effects is unknown. Because nucleolin is involved in many aspects of cell growth, proliferation, and apoptosis, knowledge of a putative target protein does not necessarily identify the processes that are affected by GROs. Further information regarding the pathways affected by GROs would facilitate the design of agents that act by a similar mechanism that may be even more active or have improved pharmacological features, compared with oligonucleotides. Therefore, in this study we proceeded to explore the

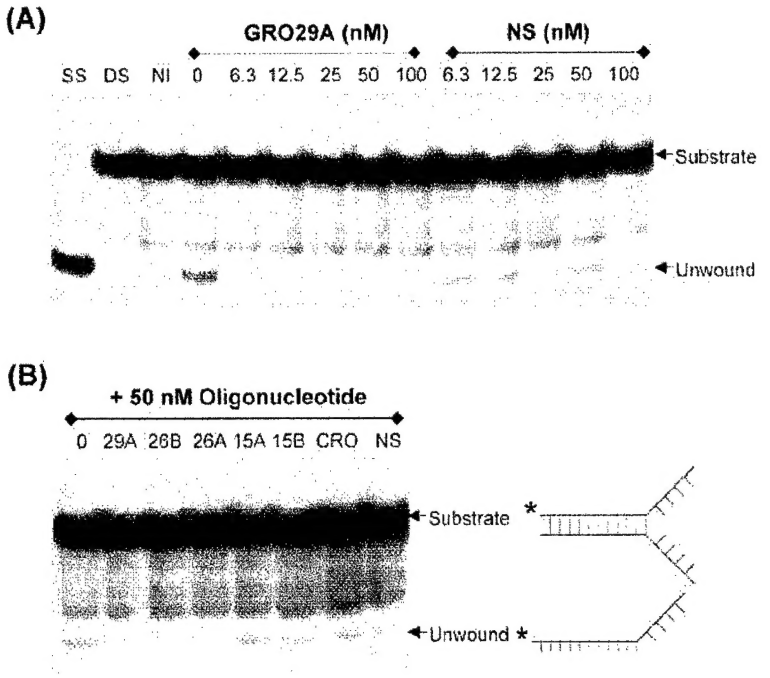


FIG. 8. *A*, helicase assay showing unwinding by SV40 large T antigen of a synthetic oligonucleotide substrate representing a replication fork. Lanes marked *SS* and *DS* are markers representing unwound (single strand 55A) and wound (partial duplex 55A/B) substrate in the absence of T antigen. *NI* is a "no incubation" control lane containing substrate and T antigen without incubation at 37 °C. In all other lanes, the helicase reaction was allowed to proceed for 15 min at 37 °C without competitor (*0*) or in the presence of unlabeled competitor oligonucleotides 29A or NS at the concentrations shown. *B*, helicase assay showing inhibition of substrate unwinding by T antigen in the presence of 50 nM concentration of competitor oligonucleotide, as indicated.

mechanism of GROs by examining their effects on cellular processes.

The conclusions of our studies are that treatment of cells with antiproliferative GRO29A causes an arrest of cell cycle progression in S phase and an inhibition of DNA replication. Because DNA synthesis is affected before RNA and protein synthesis, we have concluded that this is a primary cause of proliferation inhibition. Furthermore, because GROs can also inhibit DNA replication in a cell-free assay, we infer that the action of the GROs results directly from an effect on a protein (or proteins) involved in DNA replication. To investigate the hypothesis that GRO effects are mediated by an inhibition of DNA synthesis, we have used an *in vitro* DNA replication assay. This assay is based on the replication of a 7.4-kilobase pair circular genome that contains an SV40 origin of replication (*ori*), originally described by Li and Kelly (29, 30) and modified by Roberts and Kunkel (31). The reaction is initiated by SV40 large T antigen, which is required to recognize and unwind the *ori*. Proteins in human cell extracts carry out all subsequent steps. Inhibition of replication by GRO29A could be mediated either by damaging the template or by modulating the activity of a protein (or proteins) that is required for replication. The former mechanism is unlikely, because the replication products of damaged templates show severe inhibition of form I DNA but relatively greater amounts of nicked and linear DNA (32, 43). The GRO29A examined in this study severely inhibited the synthesis of all forms of DNA, suggesting interference with the proper function of the complex that carries out DNA replication (known as the replisome or synthesome). Therefore, we investigated the effects of GRO29A on the replication-associated proteins most likely to be modulated. These were the SV40 large T antigen, which is known to bind to and unwind G-quartet structures (42), and RPA, which is known to bind to nucleolin (20), the putative GRO-binding protein (9). Although we could observe the interaction between nucleolin and RPA, we found that this was not significantly affected by the presence of GROs. On the other hand, the ability of T antigen to unwind a synthetic substrate representing a replication fork was strongly inhibited by GRO29A. Moreover, for a series of six oligonucleotides, the relative activity in inhibiting T antigen helicase mirrored the relative activity in inhibiting DNA replication *in vitro* and also in inhibiting tumor cell proliferation. Therefore, it would appear that the antiproliferative effects of GROs on cancer cells are mediated by inhibition of DNA replication, which in turn may be related to inhibition of helicase activity. Of course, SV40 T antigen is not normally present in human cells, but GRO29A could also be an inhibitor of a human replicative helicase, which will most likely share similar features with the viral T antigen. The identity of the human replicative helicase is still not certain, but a hexameric complex of proteins known as minichromosome maintenance has been reported to have helicase activity *in vitro* and is generally thought to be a good candidate (44, 45). The ability of this complex to bind to or unwind G-quartets has not yet been reported.

G-quartet unwinding has been described previously (46–48) for a number of helicases, but to our knowledge, this is the first report that the presence of G-quartet structures can prevent a replicative helicase unwinding its double-stranded substrate. Inhibition of helicase activity has been reported for several DNA-binding agents, including many antitumor antibiotics such as anthracyclines (49–56). In these cases, it is most likely that inhibition is caused by the formation of a strong complex between the DNA-binding ligand and the template DNA, which impede the action of the helicase (49). There is considerable evidence that inhibition of helicase activity by such compounds may play some role in their anticancer activity (57), but the effect of helicase inhibition in cancer cells has not been extensively studied.

Nucleolin has been identified by us as a GRO-binding protein (9), and by several other groups (58–61) as a G-quartet-binding protein. Although the results in this paper do not clearly define a link between the molecular effects of GROs and their binding to nucleolin, they point to an effect by inhibition of helicase activity and DNA replication. Therefore, it is interesting to note that nucleolin itself has been reported to have helicase activity and is also known as DNA helicase IV (12, 22). In addition, nucleolin has been shown to interact with at least three components of the DNA replisome complex, namely RPA

(20), topoisomerase I (62), and poly(ADP-ribose) polymerase (63).

Our future studies will focus on identification of cellular helicases that may be inhibited by GRO29A, as well as clarification of the role of nucleolin in GRO activity. Such studies could lead to valuable insights into the role of nucleolin in DNA replication, as well as further elucidation of the molecular mechanisms of GRO effects.

*Acknowledgment*—We thank Virna Dapic for assistance with flow cytometry.

REFERENCES


1. Gewirtz, A. M., Sokol, D. L., and Ratajczak, M. Z. (1998) *Blood* **92,** 712–736
2. Crooke, S. T. (2000) *Methods Enzymol.* **313,** 3–45
3. Praseuth, D., Guieysse, A. L., and Helene, C. (1999) *Biochim. Biophys. Acta* **1489,** 181–206
4. Mann, M. J., and Dzau, V. J. (2000) *J. Clin. Invest.* **106,** 1071–1075
5. Gold, L. (1995) *J. Biol. Chem.* **270,** 13581–13584
6. Hermann, T., and Patel, D. J. (2000) *Science* **287,** 820–825
7. Burgess, T. L., Fisher, E. F., Ross, S. L., Bready, J. V., Qian, Y. X., Bayewitch, L. A., Cohen, A. M., Herrera, C. J., Hu, S. S., Kramer, T. B., Lott, F. D., Martin, F. H., Pierce, G. F., Simonet, L., and Farrell, C. L. (1995) *Proc. Natl. Acad. Sci. U. S. A.* **92,** 4051–4055
8. Benimetskaya, L., Berton, M., Kolbanovsky, A., Benimetsky, S., and Stein, C. A. (1997) *Nucleic Acids Res.* **25,** 2648–2656
9. Bates, P. J., Kahlon, J. B., Thomas, S. D., Trent, J. O., and Miller, D. M. (1999) *J. Biol. Chem.* **274,** 26369–26377
10. Derenzini, M., Sirri, V., Trere, D., and Ochs, R. L. (1995) *Lab. Invest.* **73,** 497–502
11. Sirri, V., Roussel, P., and Hernandez-Verdun, D. (2000) *Micron* **31,** 121–126
12. Tuteja, R., and Tuteja, N. (1998) *Crit. Rev. Mol. Biol.* **33,** 407–436
13. Ginisty, H., Sicard, H., Roger, B., and Bouvet, P. (1999) *J. Cell Sci.* **112,** 761–772
14. Srivastava, M., and Pollard, H. B. (1999) *FASEB J.* **13,** 1911–1922
15. Ginisty, H., Amalric, F., and Bouvet, P. (1998) *EMBO J.* **17,** 1476–1486
16. Kibbey, M. C., Johnson, B., Petryshyn, R., Jucker, M., and Kleinman, H. K. (1995) *J. Neurosci. Res.* **42,** 314–322
17. Lee, C. H., Chang, S. C., Chen, C. J., and Chang, M. F. (1998) *J. Biol. Chem.* **273,** 7650–7656
18. Waggoner, S., and Sarnow, P. (1998) *J. Virol.* **72,** 6699–6709
19. Gotzmann, J., Eger, A., Meissner, M., Grimm, R., Gerner, C., Sauermann, G., and Foisner, R. (1997) *Electrophoresis* **18,** 2645–2653
20. Daniely, Y., and Borowiec, J. A. (2000) *J. Cell Biol.* **149,** 799–810
21. Léger-Silvestre, I., Gulli, M. P., Noaillac-Depeyre, J., Faubladier, M., Sicard, H., Caizergues-Ferrer, M., and Gas, N. (1997) *Chromosoma* **105,** 542–552
22. Tuteja, N., Huang, N. W., Skopac, D., Tuteja, R., Hrvatic, S., Zhang, J., Pongor, S., Joseph, G., Faucher, C., Almaric, F., and Falasci, A. (1995) *Gene (Amst.)* **160,** 143–148
23. Larrucea, S., Gonzalez-Rubio, C., Cambronero, R., Ballou, B., Bonay, P., Lopez-Granados, E., Bouvet, P., Fontan, M. F., and Lopez-Trascas, M. (1998) *J. Biol. Chem.* **273,** 31718–31725
24. Callebout, C., Blanco, J., Benkirane, N., Krust, B., Jacotot, E., Guichard, G., Seddiki, N., Svab, J., Dam, E., Muller, S., Briand, J.-P., and Hovanessian, A. G. (1998) *J. Biol. Chem.* **273,** 21988–21997
25. Semenkovich, C. F., Ostlund, R. E., Olson, M. O., and Wang, J. W. (1990) *Biochemistry* **29,** 9708–9713
26. Hovanessian, A. G., Puvion-Dutilleul, F., Nisole, S., Svab, J., Perret, E., Deng, J. S., and Krust, B. (2000) *Exp. Cell Res.* **261,** 312–328
27. Dumler, I., Stepanova, V., Jerke, U., Mayboroda, O. A., Vogel, F., Bouvet, P., Tkachuk, V., Haller, H., and Gulba, D. C. (1999) *Curr. Biol.* **9,** 1468–1476
28. Sorokina, E. A., and Kleinman, J. G. (1999) *J. Biol. Chem.* **274,** 27491–27496
29. Li, J. J., and Kelly, T. J. (1984) *Proc. Natl. Acad. Sci. U. S. A.* **81,** 4249–4258
30. Li, J. J., and Kelly, T. J. (1985) *Mol. Cell. Biol.* **5,** 1238–1246
31. Roberts, J. D., and Kunkel, T. A. (1988) *Proc. Natl. Acad. Sci. U. S. A.* **85,** 7064–7068
32. McGregor, W. G., Wei, D., Maher, V. M., and McCormick, J. J. (1999) *Mol. Cell. Biol.* **19,** 147–154
33. Morgan, D. M. (1998) *Methods. Mol. Biol.* **79,** 179–183
34. Veaute, X., Mari-Giglia, G., Lawrence, C. W., and Sarasin, A. (2000) *Mutat. Res.* **459,** 19–28
35. Haider, S. R., Juan, G., Traganos, F., and Darzynkiewicz, Z. (1997) *Exp. Cell Res.* **234,** 498–506
36. Jensen, P. O., Larsen, J., Christiansen, J., and Larsen, J. K. (1993) *Cytometry* **14,** 455–458
37. Stahl, H., Droge, P., and Knippers, R. (1986) *EMBO J.* **5,** 1939–1944
38. Stahl, H., Droge, P., Zentgraf, H., and Knippers, R. (1985) *J. Virol.* **54,** 473–482
39. Malkas, L. H. (1998) *J. Cell. Biochem.* **31,** (suppl.) 18–29
40. Waga, S., and Stillman, B. (1994) *Nature* **369,** 207–212
41. Waga, S., Bauer G., and Stillman, B. (1994) *J. Biol. Chem.* **269,** 10923–10934
42. Baran, N., Pucshansky, L., Marco, Y., Benjamin, S., and Manor, H. (1997) *Nucleic Acids Res.* **25,** 297–303
43. Thomas, D. C., and Kunkel, T. A. (1993) *Proc. Natl. Acad. Sci. U. S. A.* **90,** 7744–7748
44. Tye, B. K. (1999) *Annu. Rev. Biochem.* **68,** 649–686
45. Labib, K., and Diffley, J. F. (2001) *Curr. Opin. Genet. Dev.* **11,** 64–70
46. Sun, H., Karow, J. K., Hickson, I. D., and Maizels, N. (1998) *J. Biol. Chem.* **273,** 27587–27592
47. Sun, H., Bennett, R. J., and Maizels, N. (1999) *Nucleic Acids Res.* **27,** 1978–1984
48. Fry, M., and Loeb, L. A. (1999) *J. Biol. Chem.* **274,** 12797–12802
49. Bachur, N. R., Lun, L., Sun, P. M., Trubey, C. M., Elliott, E. E., Egorin, M. J., Malkas, L., and Hickey, R. (1998) *Biochem. Pharmacol.* **55,** 1025–1034
50. Bachur, N. R., Yu, F., Johnson, R., Hickey, R., Wu, Y., and Malkas, L. (1992) *Mol. Pharmacol.* **41,** 993–998
51. Tuteja, N., and Phan, T. N. (1998) *Biochem. Biophys. Res. Commun.* **244,** 861–867
52. Tuteja, N., Phan, T. N., Tuteja, R., Ochem, A., and Falaschi, A. (1997) *Biochem. Biophys. Res. Commun.* **236,** 636–640
53. George, J. W., Ghate, S., Matson, S. W., and Besterman, J. M. (1992) *J. Biol. Chem.* **267,** 10683–10689
54. Maine, I. P., Sun, D., Hurley, L. H., and Kodadek, T. (1992) *Biochemistry* **31,** 3968–3975
55. Chino, M., Nishikawa, K., Yamada, A., Ohseno, M., Sawa, T., Hanaoka, F., Ishizuka, M., and Takeuchi, T. (1998) *J. Antibiot. (Tokyo)* **51,** 480–486
56. Zhu, K., Henning, D., Iwakuma, T., Valdez, B. C., and Busch, H. (1999) *Biochem. Biophys. Res. Commun.* **266,** 361–365
57. Gewirtz, D. A. (1999) *Biochem. Pharmacol.* **57,** 727–741
58. Hanakahi, L. A., Sun, H., and Maizels, N. (1999) *J. Biol. Chem.* **274,** 15908–15912
59. Dempsey, L. A., Sun, H., Hanakahi, L. A., and Maizels, N. (1999) *J. Biol. Chem.* **274,** 1066–1071
60. Dickinson, L. A., and Kohwi-Shigematsu, T. (1995) *Mol. Cell. Biol.* **15,** 456–465
61. Ishikawa, F., Matunis, M. J., Dreyfuss, G., and Cech, T. R. (1993) *Mol. Cell. Biol.* **13,** 4301–4310
62. Bharti, A. K., Olson, M. O., Kufe, D. W., and Rubin E. H. (1996) *J. Biol. Chem.* **271,** 1993–1997
63. Borggrefe, T., Wabl, M., Akhmedov, A. T., and Jessberger, R. (1998) *J. Biol. Chem.* **273,** 17025–17035